Deformation effects in layer crystals

G. L. Belen'kiĭ, É. Yu. Salaev, and R. A. Suleĭmanov

Institute of Physics, Academy of Sciences of the Azerbaidzhan SSR, Baku
Usp. Fiz. Nauk **155**, 89–127 (May 1988)

A unit cell of a layer crystal may contain several layers and the atoms in these layers may interact with one another in different ways. The dependences of the forces of the interaction between the atoms on the distances separating them are also different. The deformation effects in crystals of this kind are unusual. This review reports experimental results obtained in studies of vibrational and electronic spectra of graphite and of layer semiconductors (mainly III-VI compounds) under conditions of elastic deformation at various temperatures. An analysis is made of the results of experimental investigations of thermal expansion of layer crystals. In each case a discussion is given of models which, on the whole, can provide a satisfactory explanation of the nature of the characteristic features of the observed effects.

CONTENTS

1. INTRODUCTION

Experimental and theoretical investigations of the energy spectra of deformed crystals carried out in the last few decades have proved to be extremely fruitful in the establishment of a full picture of these spectra. The behavior of the electron and phonon states in a crystal in which atoms are bound by very different forces can be unusual in a deformed state because the binding forces between the atoms in a unit cell depend differently on the distances between them.

It has now become clear that the anisotropy of the binding forces in a crystal is manifested in different ways in the properties of different phonon and electron states.[1] For example, the phonons corresponding to the displacements of atoms bound by a strong interaction are characterized by a low dispersion in the direction of a weak interaction. The frequencies of such phonons are high. Layer crystals are characterized also by low-frequency optical phonons corresponding to vibrations of layers relative to one another, as if they were rigid molecules. The acoustic spectra of layer crystals are also unusual and the law of dispersion of waves traveling along the layer planes and polarized at right-angles to these planes differs from the usual linear law and includes a quadratic term. The anisotropy of vibrational spectra of layer crystals is therefore strong. On the other hand, in the case of semiconductors of the GaSe type the electron states near the top of the valence band and the bottom of the conduction band are characterized by a strong dispersion along all the directions in the Brillouin zone, i.e., these states are "three-dimensional." Two-dimensional states lie well inside the valence band. They are characterized by a strong anisotropy of the effective masses and by narrow energy bands along the relevant directions.

In this review we shall consider a number of deformation effects characteristic of vibrational and electronic properties of layer crystals. In the second section we use the examples of different layer crystals to demonstrate the characteristics of their structure, elastic properties, and features of vibrational spectra. We shall show that a strong anisotropy of the binding forces in a crystal makes it necessary to review the conditions of validity of certain approximations used in the description of elastic properties and vibrational spectra of crystals. For example, the experimentally observed quadratic dispersion laws of acoustic waves traveling in the planes of the layers and polarized at right-angles to the layers can be explained provided we allow not only for the interaction between the nearest neighbors in the planes of the layers, but also between the more distant atoms. In the same section we shall describe the most striking deformation effects associated with optical vibrations in layer crystals. The lines in the Raman scattering spectra of layer crystals shift in different ways on the application of a pressure p and

 0038-5670/88/050434-22$01.80

the mode parameters

$$\Gamma_\omega = \frac{1}{\omega}\frac{d\omega}{dp}$$

for different frequencies ω are very different. An analysis of the corresponding displacement vectors of normal vibrations makes it possible to understand the reason for this difference, which is associated with the presence of two types of binding (strong and weak) in a unit cell of a layer crystal.

In discussing thermal expansion of any crystal we generally have to consider normal modes of a deformed lattice. The third section of the present review therefore deals with the characteristic features of thermal expansion of layer crystals. The available experimental data on the temperature dependences of the components of the thermal expansion tensor make it possible to identify a common feature of a number of crystals, which is the existence of a range of temperatures in which the linear expansion coefficient along the layers $\alpha_\parallel$ can have negative values. We shall consider the results of a quantitative description of the temperature dependences of the thermal expansion coefficients of layer crystals of C, BN, and GaS using a model proposed by I. M. Lifshitz.[2] The model allows for the fact that the anisotropy of the binding forces gives rise to special dispersion laws and high densities of states of transverse acoustic waves propagating in the planes of the layers and involving transverse atomic displacements (flexural waves). These waves exhibit a characteristic deformation effect: their frequency rises as a crystal expands in the plane of the layers and this is known as the membrane effect. A suitable selection of the temperature interval can ensure predominance of waves of this type and such an interval exhibits a negative linear expansion of a crystal.

The last (fourth) section deals with the experimental pressure dependences of the widths of the band gap of layer semiconductors recorded at different temperatures, particularly in crystals of the GaSe type. When pressure is varied at $T = \text{const}$ or when temperature is varied when $p = \text{const}$ the pressure coefficients of the various direct and indirect band gaps of these crystals not only vary in respect of the magnitude, but also in respect of the sign. An analysis of the available data on the energy band structure of crystals of the GaSe type makes it possible to consider a model of the shift of the electron energy bands of layer crystals with pressure, which allows not for the deformation of a unit cell as a whole, but for changes in the intralayer and interlayer distances separately. In this case the deformation potential describing the change in the energy of an electron level with pressure consists of two terms which have different signs and which vary with temperature and pressure in accordance with the temperature and pressure dependences of the components of the strain tensor. In a certain range of pressures and temperatures the conditions may be such that the sign of the pressure coefficient changes with pressure at a fixed temperature or changes with temperature when the pressure is fixed.

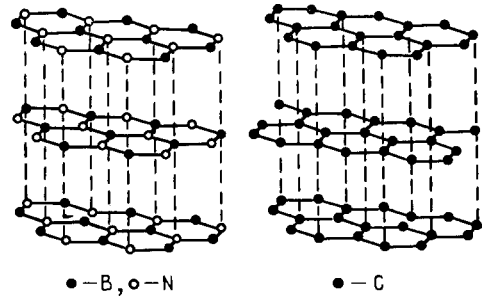

FIG. 1. Crystal structures of graphite (C) and boron nitride (BN).

The pressure dependences of the electron energy bands of layer crystals can in most cases be explained on the basis of the published band structure calculations. The characteristics of pressure dependences are influenced in a major way by the nature of a given state, and by whether this state is formed as a result of a significant participation of atoms governing the interlayer interaction or whether an important role is played by those atoms which are responsible for the strong binding within the layers.

2. VIBRATIONAL SPECTRA AND ELASTIC PROPERTIES OF LAYER CRYSTALS. INFLUENCE OF PRESSURE AND TEMPERATURE

2.1. Crystal structure and elastic properties of layer crystals

It is now known that there are many crystals with a layer structure of the lattice.[3] The simplest structures are those of graphite[4] and boron nitride[5] (Fig. 1). The lattices of these crystals are composed of two-dimensional series of hexagons with atoms at the vertices. The distances between the atoms in the planes of the layers are considerably smaller than the interlayer distances. In graphite the atoms in a layer are separated by a distance of 1.421 Å, whereas the distances between the layers are 3.3 Å; similarly in the case of boron nitride we have 1.446 and 3.33 Å. All layer crystals have similar structures, but a layer in each of them contains three

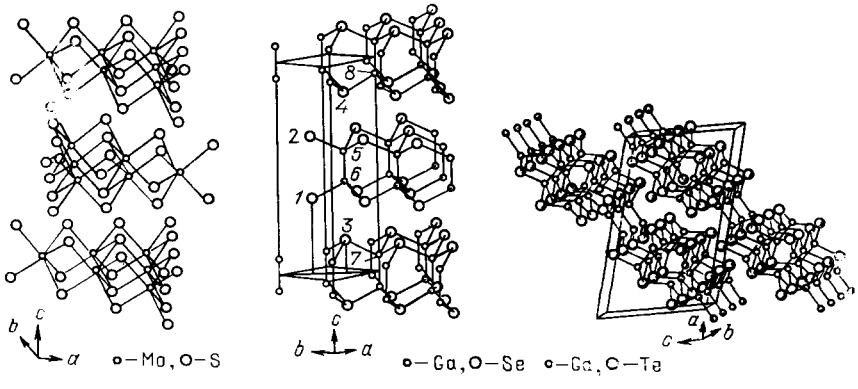

FIG. 2. Crystal structures of layer semiconductors MoS_2, GaSe, and GaTe (not to scale).

TABLE I. Lattice parameters and atomic spacings (Å) in III–VI layer crystals (the atoms are labeled as in Fig. 1).

Crystal	GaSe (Ref. 6)				GaS (Ref. 7)	InSe (Ref. 8)
Polytype	β	ε	γ	δ	β	ε
$(S, Se)_2-(In, Ga)_5$, inside layers	2,515	2,485	2,467	2,463	2,322	2,53
$(In, Ga)_5-(In, Ga)_6$, inside layers	2,391	2,383	2,386	2,457	2,44	3,16
$(S, Se)_1-(S, Se)_2$, inside layers	4,491	4,766	2,722	4,784	4,54	4,82
$(S, Se)_1-(S, Se)_3$, between layers	4,199	3,840	8,847	3,890	3,81	4,19
a	3,755	3,755	3,739	3,755	3,585	4,05
c	15,95	15,996	23,862	31,99	15,53	16,93

or more atomic planes. Figure 2 shows the layer crystal structures of some binary semi-conductor compounds. The distances between the layers in all such crystals are almost the same as in graphite, but the distances between the atoms in a layer are somewhat greater. Weakly bound layers with the same structure form a three-dimensional crystal. The contacts between layers may vary and the layer crystals usually exhibit polytypism. Since the attention will be concentrated mainly on layer III–VI semiconductor compounds, we shall consider their structure in greater detail. The structure of the layers in GaSe, GaS, and InSe is the same. Atomic planes in the layers are oriented at right-angles to the layers (along a symmetry axis) in the following sequence: anion-cation-anion (for example, in the case of GaSe this sequence is Se–Ga–Ga–Se). The space symmetry group of a layer in all three crystals is D^1_{3h} ($6m2$). Gallium selenide crystallizes. in four different polytypes. The polytype β has the space symmetry group D^4_{6h} ($6/mm$) and contains two layers in a unit cell, which is also true of the ε polytype with the space symmetry group D^1_{3h}. The γ polytype has the rhombohedral structure with C^5_{3v} ($3m$) and three layers in a unit cell, whereas the hexagonal δ polytype is characterized by C^4_{6v} ($6mm$) and has four layers in a unit cell.

Gallium sulfide crystallizes only in the β structure, whereas indium selenide can have the ε or γ structure. Table I gives the data on the unit cell parameters and interatomic distances in various III–VI semiconductor compounds.

The experimental data on changes in the structure of layer crystals under the application of pressure are rather scarce. The transformation of x-ray diffraction patterns of polycrystalline samples of gallium sulfide under the action of hydrostatic pressures is attributed in Ref. 9 to a phase transition at 18 kbar. It is assumed that this is a first-order transition $\beta \rightarrow \varepsilon$. The fullest investigation of the influence of pressure (right up to 65 kbar) on the crystal structure of gallium sulfide is reported in Ref. 7. Figure 3 shows the crystal structure of GaS at atmospheric pressure and at 30 kbar. The main difference between these two structures is a change in the number of sulfur atoms surrounding Ga atoms in the second configuration sphere. At atmospheric pressure the number of such atoms is 4, whereas at 30 kbar this number is 6. Before and after the phase transition the space symmetry group is the same (D^4_{6h}) and the distances between gallium atoms within the layers change only slightly (2.44–2.38 Å), whereas those between the layers decrease significantly from 3.81 to 3.36 Å. The difference between the atomic distances within the layers and between the layers reflect the anisotropy of the binding forces in layer crystals. This is manifested by the magnitudes of the elastic constants representing the elastic properties of layer crystals.

A weak deformation of a solid considered in the theory of elasticity is described by the strain tensor

$$u_{ik} = \frac{1}{2}\left(\frac{\partial u_i}{\partial x_k} + \frac{\partial u_k}{\partial x_i}\right);$$

here, u_i is a component of the displacement vector. The internal stresses which arise in the course of deformation are described by the stress tensor σ_{ik}. The tensor σ_{ik} is defined by

$$F_i = \frac{\partial \sigma_{ik}}{\partial x_k},$$

where F_i is the component of the force acting per unit volume. The strain and stress tensors are symmetric and of second rank. The diagonal components of the strain tensor describe the relative changes in distances along relevant directions, whereas the off-diagonal components describe shear strains.

The relationship between the stress and strain tensors is known as Hooke's law:

$$\sigma_{ik} = C_{iklm} u_{lm}. \tag{2.1}$$

The fourth-rank tensor C_{iklm} is known as the elasticity tensor and its components are called the elastic moduli or the elastic constants. The requirement of the symmetry of the stress and strain tensors leads to equality of many of the elastic constants. The relationship

$$C_{iklm} = C_{lmik} = C_{kilm} = C_{ikml}$$

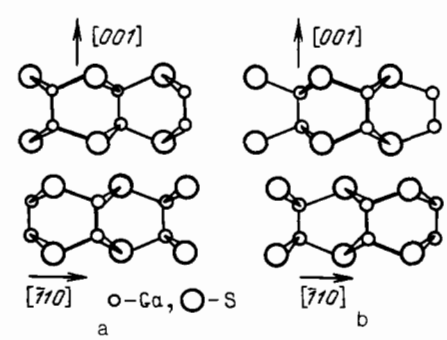

FIG. 3. Structure of GaS at atmospheric pressure (a) and at the pressure of 30 kbar (b, Ref. 7). View along the [110] direction.

reduces the number of different elastic constants of a crystal to 21. An allowance for the symmetry of the specific crystal lattice reduces still further the number of independent elastic constants. A completely isotropic solid has two elastic constants, cubic crystals have three constants, and crystals with the hexagonal symmetry typical of many layer crystals are described by five elastic constants:

$$C_{xxxx} = C_{yyyy},\ C_{zzzz},\ C_{xxzz} = C_{yyzz},\ C_{xxyy},\ C_{xzxz} = C_{yzyz}.$$

The symmetry of the elasticity tensor C_{iklm} makes it possible to adopt compact notation. We shall use the following compact notation system: $xx \to 1$, $yy \to 2$, $zz \to 3$, $yz \to 4$, $xz \to 5$, $xy \to 6$. A hexagonal crystal is characterized by elastic constants C_{11}, C_{12}, C_{33}, C_{13}, and C_{44}, the values of which govern its anisotropy. For example, in the case of a layer crystal with the symmetry axis perpendicular to the layers the elastic constants C_{11} and C_{12} represent the binding inside the layers, whereas the constants C_{33}, C_{13}, and C_{44} determine largely the interlayer binding. The elastic properties of a hexagonal crystal in a symmetry plane are isotropic and are described by two constants C_{11} and C_{12}, which determine the Young's modulus and the Poisson ratio in the symmetry plane. The constant C_{33} governs the Young's modulus in the perpendicular direction, whereas the constants C_{13}, C_{11}, C_{12}, and C_{33} determine the corresponding Poisson ratio. The constant C_{44} represents the stresses which appear in a hexagonal crystal as a result of shear in the basal plane, and the value of C_{44} for a layer crystal describes the stresses which occur when layers shear relative to one another. The physical meaning of the other elastic constants can be deduced also from the expressions for the diagonal components of the strain tensor obtained for different types of deformation. We shall give the relevant expressions for the cases of uniaxial deformation of a symmetry axis and at right-angles to such an axis, and also in the case of hydrostatic compression:

uniaxial compression parallel to a symmetry axis (z axis):

$$u_{zz} = -\frac{C_{11}+C_{12}}{(C_{11}+C_{12})\cdot C_{33}-2C_{13}^2}\,p,$$
$$u_{xx} = u_{yy} = \frac{C_{13}}{(C_{11}+C_{12})C_{33}-2C_{13}^2}\,p; \qquad (2.2)$$

uniaxial compression perpendicular to the z axis:

$$u_{zz} = -\frac{C_{13}}{(C_{11}+C_{12})C_{33}-2C_{13}^2}\,p,$$
$$u_{xx}+u_{yy} = -\frac{C_{33}}{(C_{11}+C_{12})C_{33}-2C_{13}^2}\,p; \qquad (2.3)$$

hydrostatic compression:

$$u_{zz} = -\frac{C_{11}+C_{12}-2C_{13}}{(C_{11}+C_{12})C_{33}-2C_{13}^2}\,p,$$
$$u_{xx} = u_{yy} = -\frac{C_{33}-C_{13}}{(C_{11}+C_{12})C_{33}-2C_{13}^2}\,p. \qquad (2.4)$$

A strong anisotropy of the elastic properties of a layer crystal implies the inequalities

$$C_{11},\ C_{12} \gg C_{13},\ C_{33},\ C_{44}.$$

It readily follows from Eqs. (2.2)–(2.4) that in this case there is a large difference between the Young's moduli and Poisson ratios for the basal plane and at right-angles to this plane. Comparison of Eqs. (2.2) and (2.4) also shows that in the case of a strongly anisotropic crystal the relative elongation along the symmetry axis under hydrostatic pressure is practically identical with the elongation in the case of a uniaxial compression parallel to the z axis. This is important in the interpretation of the deformation effects in layer crystals.

We shall consider the experimentally determined values of the elastic constants of a number of layer crystals with hexagonal symmetry.

Graphite has been investigated more thoroughly than the other materials. The data on the elastic constants of this crystal have been obtained by investigations of the compressibility,[10] neutron scattering,[11] and velocity of ultrasound,[12] and by calculations of the specific heat.[13,14] The elastic constants of the same samples have been determined by different methods in (Ref. 15). The experimental data taken as a whole demonstrate a strong dependence of the value of C_{44} for graphite on the conditions of crystal growth. For example, it is shown in Ref. 16 that a reduction in the number of basal dislocations increases C_{44} significantly. The elastic constants of GaS have been determined by the methods of neutron scattering,[15] light scattering,[18–20] and ultrasound propagation.[21] In the case of GaSe, investigations have been made of the scattering of light[19–23] and the velocity of propagation of sound.[24,25] In the case of InSe the elastic properties have been determined by the ultrasonic method.[21,26] Table II gives the elastic constants of graphite, III–VI crystals, and some other layer semiconductors. We can see that the strongest anisotropy of the elastic constants is exhibited by graphite and the anisotropy of the constants of other crystals is considerably less.

Serious difficulties are encountered in the determination of the elastic constants of layer crystals. The most popular method involves determination of the velocities of propagation of ultrasound along various crystallographic

TABLE II. Elastic constants of layer crystals (10^{11} dyn/cm^2).

Elastic constant	Hexagonal crystals				Rhombohedral crystals			
	C (Ref. 15)	GaS (Ref. 19)	GaSe (Ref. 21)	InSe (Ref. 21)	$TiSe_2$ (Ref. 27)	$TaSe_2$ (Ref. 28)	$NbSe_2$ Ref. 28)	$SnSe_2$ (Ref. 29)
C_{11}	106	15,7	10,3	7,3	12	22,9	19,4	10,3
C_{12}	18	3,3	2,9	2,7	4,2	10,7	9,1	—
C_{13}	1,5	1,5	1,2	3,0	—	—	—	—
C_{33}	3,7	3,6	3,4	3,6	3,9	5,4	4,2	2,8
C_{44}	0,018—0,035	0,8	0,9	1,2	1,4	1,9	1,8	1,8

TABLE III. Pressure dependences of elastic constants of layer crystals.

Crystal	Pressure, kbar	$\frac{1}{C_{ik}}\frac{\partial C_{ik}}{\partial p}$, 10^{-11} dyn/cm^2					Ref.
		C_{11}	C_{12}	C_{33}	C_{13}	C_{44}	
C	$p\|c$, up to 0.42 kbar	—	—	9±2	—	—	15
	hydrostatic, 7 kbar	—	—	3,9	—	1,4	30
GaS	hydrostatic, 20 kbar	0,4	0,6	2,6	2,1	0,8	31
	hydrostatic, 20 kbar	0,4	—	2,8	—	—	32
	hydrostatic, 3 kbar	0,7	1,5	6,0	—	—	21
GaSe	hydrostatic, 3 kbar	0,8	1,5	5,6	—	—	21
InSe	hydrostatic, 3 kbar	1,0	1,6	5,0	—	—	21

directions. For example, the value of C_{13} can be determined when a sample has faces polished at an angle to the planes of the layers, which is difficult to achieve in practice. For this reason the values of C_{13} determined by different authors can be quite different. The quality of a crystal may also have a very important influence on the elastic constants. For example, the value of C_{44} for graphite can vary within wide limits (Table II), depending on the number of defects formed as a result of incorrect sequencing of layers relative to one another.

In later sections of this review we shall show that the characteristics of the deformation effects in layer crystal are determined to a great extent by the pressure and temperature dependences of the elastic constants. Determination of the values of C_{ik} in the presence of external perturbations meets with additional experimental difficulties. This is the reason for the small number of investigations of the influence of pressure and temperature on the elastic properties of layer crystals. Table III gives the results of the published studies of changes in C_{ik} with pressure in the case of graphite and GaSe, GaS, and InSe crystals. The data on graphite[15,30,31] have been obtained from investigations of the velocity of propagation of ultrasound under conditions of uniaxial compression parallel to the z axis and under hydrostatic pressure. The value of C_{11} has been determined by measuring the velocity of propagation of longitudinal waves in the plane of the layers, whereas C_{33} has been deduced from the velocity of longitudinal waves traveling along the symmetry axis. The values of C_{12} and C_{44} have been deduced from the velocities of transverse waves propagating along and across the layers, respectively. For the reasons given above the value of C_{13} has not been determined directly, but has been estimated from the results of a number of reported measurements and on the basis of certain assumptions.

The main result of an analysis of the data in Table III is that the pressure dependences of the interlayer elastic constants are stronger than the pressure dependences of the intralayer constants.

An analysis of the data on the temperature dependences of the elastic constants of graphite[31] also reveals a tendency for the faster changes in the interlayer elastic constants, compared with the intralayer constants. For example, cooling from 300 to 4.2 K increases C_{11} by 6%, whereas C_{33} increases by 12%. The faster rise on reduction in temperature and on increase in pressure exhibited by the interlayer elastic constants is not surprising. In the case of crystals formed from rare gases and molecular crystals, where the binding between atoms is of the van der Waals nature, the elastic constants vary faster with pressure and temperature than the majority of ordinary semiconductors.[33] The same result follows from an analysis of the temperature dependences of the frequencies of optical phonons in layer crystals, which is given below (Sec. 2.3).

The elastic constants carry information on the nature of the forces of interaction between the atoms composing a crystal. We can establish a relationship between the experimental values of the elastic constants C_{ik} and the microscopic parameters of model calculations which determine the nature of the interaction between atoms. The elastic properties and the phonon spectra of crystals are frequently calculated using a model of force constants according to which the relationships between displacements of a given atom from its equilibrium position $\mathbf{u}(n)$ and the forces exerted on this atom by all the other atoms in the crystal lattice are written in the form

$$m\ddot{u}_i(n) = -\sum_{n'} \alpha_{ik}(n, n')\, u_k(n'); \qquad (2.5)$$

here, $u_i(n)$ is a component of the vector describing the displacement of the nth atom from its equilibrium position and α_{ik} represents elements of the force matrix of a crystal.

The interaction forces between atoms decrease quite rapidly with distance, so that a correct description of lattice dynamics in a specific crystal structure can frequently be provided by considering only the nearest neighbors. It is assumed that the interaction between atoms is of central nature, i.e., it acts along the direction of the line joining the atoms and depends only on the distance between them. These simple assumptions make it possible to describe the vibrational spectrum and many elastic properties of a crystal. On the other hand, the simple description of the crystal structure of a layer material, allowing for the existence of different binding forces within the layers and between the layers, cannot be based on the above assumptions as the first approximation. If the intralayer forces are much stronger than those between the layers, the interaction between the more distant neighbors in the basal plane may be of the same order of magnitude as that between the nearest neighbors bound by a weak interlayer force. Moreover, because the interlayer central forces are weak, an allowance for the noncentral forces of interaction between atoms in the plane of the layers may be important. Allowance for just the central forces imposes certain (Cauchy) relationships between the elastic constants[33] and in the case of a crystal of hexagonal symmetry these relationships are

$$C_{12} = C_{66} = \frac{C_{11}-C_{12}}{2}, \quad C_{13} = C_{44}. \qquad (2.6)$$

It is clear from Table II that the relationships of Eq. (2.6)

are satisfied by GaS, GaSe, and InSe. In the case of graphite the elastic constant C_{13} is almost two orders of magnitude different from the value of C_{44}. The violation of the Cauchy relationships in the case of graphite demonstates that noncentral forces must be allowed for in the case of this crystal. As demonstrated below, an analysis of the vibrational spectra of strongly anisotropic crystals on the basis of only the central interaction cannot account for all the features of the dispersion laws exhibited experimentally by such crystals.

2.2. Characteristics of the spectra of acoustic vibrations in layer crystals

In dealing with the spectrum of acoustic phonons in layer crystals we shall concentrate on the characteristics typical of acoustic vibrations in the case of extreme anisotropy of the binding forces. The dispersion laws for elastic waves in crystals follow from the equations of motion $\rho\ddot{u}_i = \partial\sigma_{ik}/\partial x_k$ and are found by equating to zero the following determinant:

$$| C_{iklm}k_k k_l - \rho\omega^2\delta_{im} | = 0; \tag{2.7}$$

here, k_k is a component of the wave vector of elastic waves, ω is the vibration frequency, and ρ is the density. Equation (2.7) has generally three different solutions $\omega(\mathbf{k})$. All three of them describe waves propagating at a velocity which is independent of the wave vector because Eq. (2.7) defines ω as a linear function with respect to the wave vector components.

We shall consider a crystal with hexagonal symmetry and assume that its elastic properties are described by the elastic constants C_{11}, C_{12}, C_{13}, C_{44}, C_{33}, and $C_{66} = (C_{11} - C_{12})/2$. In this case the solutions of Eq. (2.7) are of the form[34]

$$\begin{aligned}
\omega_1^2 &= \frac{k^2}{\rho}(C_{66}\sin^2\theta + C_{44}\cos^2\theta),\\
\omega_{2,3}^2 &= \frac{k^2}{2\rho}[(C_{11}+C_{44})\sin^2\theta + (C_{33}+C_{44})\cos^2\theta\\
&\pm \{[(C_{11}-C_{44})\sin^2\theta - (C_{33}-C_{44})\cos^2\theta]^2\\
&+ 4(C_{44}+C_{13})^2\sin^2\theta\cdot\cos^2\theta\}^{1/2}];
\end{aligned} \tag{2.8}$$

here θ is the angle between the direction of the vector $\mathbf{k}$ and the symmetry axis. If we assume a strong anisotropy of the elastic properties, i.e., $C_{33}, C_{13}, C_{44} \ll C_{11}, C_{12}$, we obtain the following dispersion laws for the three branches of the acoustic spectrum of a layer crystal[2]:

$$\begin{aligned}
\omega_1^2 &= \frac{C_{11}-C_{12}}{2\rho}(k_x^2+k_y^2) + \frac{C_{44}}{\rho}k_z^2,\\
\omega_2^2 &= \frac{C_{11}}{\rho}(k_x^2+k_y^2) + \frac{C_{44}}{\rho}k_z^2,\\
\omega_3^2 &= \frac{C_{44}}{\rho}(k_x^2+k_y^2) + \frac{C_{33}}{\rho}k_z^2.
\end{aligned} \tag{2.9}$$

In the case of a strongly anisotropic crystal each branch of these vibrations corresponds to a displacement vector oriented in a specific way: the first and second branches correspond to displacements of atoms in the plane of the layers and the third branch corresponds to displacement in the perpendicular direction. This last branch is called flexural because the layer becomes bent in its plane in the course of propagation of such vibrations. A comparison of the dispersion relationships of Eq. (2.9) with the dispersion laws of, for example, graphite found experimentally by neutron scattering spectroscopy methods, shows that the theory and experiment agree on the whole quite well. The exception is the dispersion relationship $\omega_3(\mathbf{k})$. It follows from the experimental results that in the case of the flexural branch, because of the smallness of C_{44}, the dispersion relationship must include terms quadratic in k_x and k_y even for relatively small values of k_x and k_y:

$$\omega_3^2 = \frac{C_{44}}{\rho}(k_x^2+k_y^2) + \frac{C_{33}}{\rho}k_z^2 + \gamma^2(k_x^2+k_y^2)^2.$$

The unusual behavior of the flexural branch was first predicted in 1952 by I.M. Lifshitz[2] who demonstrated the need to supplement the dispersion relationship $\omega_3(\mathbf{k})$ with a quadratic term. Lifshitz pointed out[2] that, in addition to equations of the theory of elasticity, the derivation of the dispersion relationships for strongly anisotropic crystals must allow for the restoring forces which arise as a result of bending of individual layers. The coefficient γ represents the flexural rigidity of the layers. This feature is typical also of vibrations of a string. The frequencies of short-wavelength vibrations of a string calculated without allowance for the flexural forces are considerably lower than those found experimentally.[35]

I. M. Lifshitz used the analogy between a layer in a crystal and a thin elastic plate. The transverse vibrations of such a plate are known to be described by the following quadratic dispersion law:

$$\omega^2 = \frac{Ed^2}{12\rho(1-\sigma^2)}k_\parallel^4. \tag{2.10}$$

In Eq. (2.10), E is Young's modulus, σ is the Poisson ratio, d is the thickness of the plate, and $k_\parallel$ is the wave vector lying in the plane of the plate. The coefficient $Ed^2/12(1-\sigma^2)$ represents the rigidity of the plate and its resistance to bending.

The dispersion laws for acoustic vibrations in a crystal can be derived also using the framework of a very simple model of the force constants. Such a model is considered for a layer crystal in Ref. 36.

The dispersion laws corresponding to Eq. (2.5) can be found in the model of force constants by equating to zero a determinant analogous to Eq. (2.7):

$$| \sum_{n-n'} \alpha_{im}(n, n')[\cos(\mathbf{kr}(n-n')) - 1] - m\omega^2\delta_{im} | = 0; \tag{2.11}$$

here, $\mathbf{k}$ is the wave vector and $\mathbf{r}(n)$ is the radius vector of the nth atom. It follows from Eq. (2.11) that in the long-wavelength approximation the dispersion laws are generally nonlinear. Linear dispersion laws are obtained only if we retain only the terms up to $\sim k^2$ in the expansion for the cosine and allow for the interaction of atoms with the nearest neighbors.

We shall use a simple model of the crystal structure of a layer crystal and demonstrate under what conditions the dispersion laws obtained using the framework of the theory of elasticity [Eq. (2.9)] agree with the results of microscopic calculations based on Eq. (2.11). Figure 4 shows a simplified model of the structure of graphite in which parameters of a unit cell along the symmetry axis and in the plane of the layers are equal. We shall consider the interaction of an atom 1 with the neighboring atoms 2–9 and allow only for the central interaction. We can readily show that under the as-

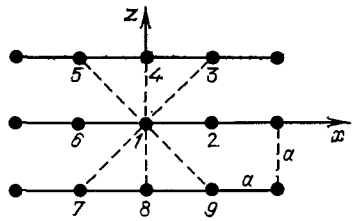

FIG. 4. Simplified structure of graphite.

sumptions made and including only the first two terms in the expansion for the cosine, the dispersion laws obtained from Eq. (2.11) are identical with the laws deduced using the theory of elasticity. For example,

$$\omega_2^2 \approx \frac{\alpha_{xx}(1,2)}{a}\frac{1}{m/a^3}(k_x^2+k_y^2)+\frac{\alpha_{xx}(1,3)}{a}\frac{1}{m/a^3}k_z^2,$$
$$\omega_3^2 \approx \frac{\alpha_{zz}(1,3)}{a}\frac{1}{m/a^3}(k_x^2+k_y^2)+\frac{\alpha_{zz}(1,4)}{a}\frac{1}{m/a^3}k_z^2. \quad (2.12)$$

The elastic constants C_{11}, C_{44}, and C_{33} are related to the force constants as follows:

$$C_{11}=\frac{\alpha_{xx}(1,2)}{a},$$
$$C_{44}=\frac{\alpha_{zz}(1,3)}{a}=\frac{\alpha_{xx}(1,3)}{a}=C_{13},\quad C_{33}=\frac{\alpha_{zz}(1,4)}{a}.$$

The dispersion law for the flexural branch is linear and the velocity of propagation of a flexural wave in the plane of the layers is governed by the central interaction of the atom 1 with atoms of the type 3, i.e., with the atoms labeled 5, 7, and 9, as well as with atoms (not shown in Fig. 4) lying in neighboring planes parallel to the (x,z) plane. It therefore follows that inclusion of just the interaction between the nearest neighbors bound by the central forces gives dispersion laws which agree with those deduced from the theory of elasticity. The shortcoming of this analysis is obvious: only the central interaction between the weakly bound atoms (1 and 3, . . .) is allowed for and the noncentral interaction between the strongly bound atoms (1 and 2, . . .) is ignored. This neglect is not justified in the case of strongly anisotropic binding forces. We shall consider the dispersion relationship for the flexural branch allowing for the noncentral interaction of atoms in the plane of the layers. In this case we can no longer limit our treatment to just the nearest neighbors. This can be demonstrated conveniently by ignoring the interaction between the layers and considering an isolated layer or chain. Then, in the discussion of the flexural vibrations the need to exclude rotation of the layers or chains as a whole leads to important relationships between the force constants describing the interaction between the nearest and the more distant neighbors. In fact, we shall assume that the chain shown in Fig. 4 is rotated as a whole in the (x,z) plane. The forces acting on each atom in the chain vanish. This also follows from Eq. (2.11): in the limit $k\to 0$ the force tends to zero. An important consequence is that rotation of the chain as a whole makes the total internal energy also zero. Therefore,

$$\sum_{n-n'}\alpha_{zz}(n,n')(n-n')^2=0. \quad (2.13)$$

Clearly, this condition can be satisfied only if the force constants $\alpha_{zz}(n,n')$ differ in sign and are not very different in absolute magnitude. The physical meaning of this conclusion is that flexural rigidity of a layer or a chain requires that a given atom interacts not only with the nearest neighbors, but also with the more distant neighbors and the binding to the more distant neighbors may be slightly weaker than that to the nearest neighbors.

The dispersion law for the flexural branch of vibrations of an isolated chain can be deduced from Eq. (2.11) allowing for Eq. (2.13):

$$m\omega_3^2=\sum_{n-n'}\alpha_{zz}(n,n')[\cos(ka(n-n'))-1]. \quad (2.14)$$

Clearly, because of Eq. (2.13) we cannot limit our treatment to the first term of the expansion of the cosine as a series. The dispersion law becomes

$$\omega_3^2 \approx \frac{\alpha_{zz}(1,2)}{m}(ak)^4. \quad (2.15)$$

In a real crystal when allowance is made for the interaction between the layers, the dispersion law for the flexural branch is of the form[36]

$$\omega_3^2=\frac{\alpha_{xx}(1,3)}{m}a^2(k_x^2+k_y^2)+\frac{\alpha_{zz}(1,2)}{m}a^4(k_x^2+k_y^2)^2+\frac{\alpha_{zz}(1,4)}{m}a^2k_z^2. \quad (2.16)$$

The above analysis of the main relationship governing the dispersion laws of a strongly anisotropic crystal allows us to draw the conclusion that the deviation of the dispersion law of the flexural branch from linearity is governed by the relationship between the strengths of the central interlayer forces and the noncentral intralayer forces. A quadratic dispersion law should be typical of crystals with very different forces of interaction within and between the layers.

We shall now consider the experimental data on the scattering of slow neutrons in layer crystals because it is this scattering method that makes it possible to reconstruct independently the dispersion relationships governing acoustic vibrations. It was found that the quadratic dispersion law for the flexural branch of vibrations typical of graphite[37] (Fig. 5) is exhibited also by MoS_2 (Ref. 38), $TiSe_2$ (Ref. 39), and GaS (Ref. 17), as demonstrated in the last case in Fig. 6. On

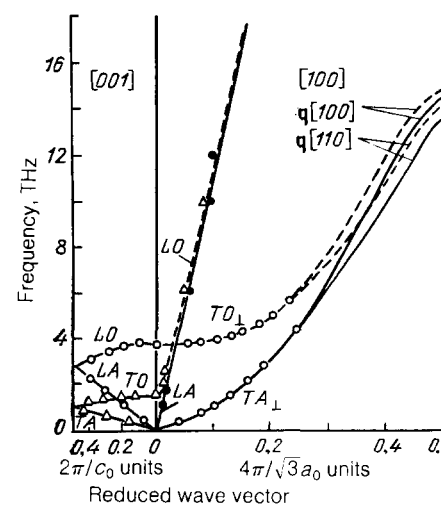

FIG. 5. Dispersion of phonons in graphite.[37]

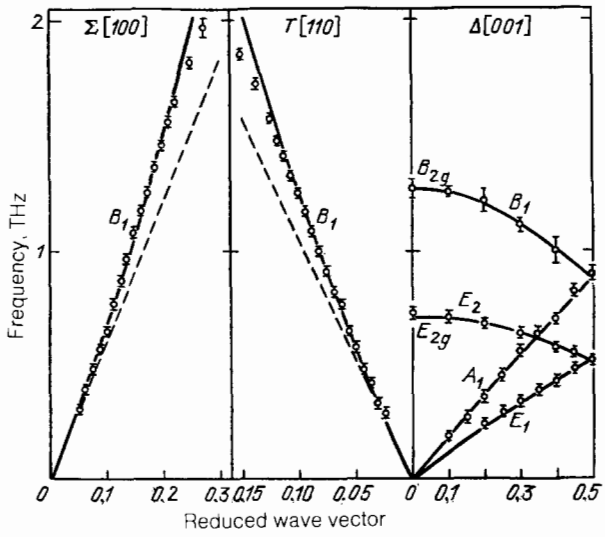

FIG. 6. Dispersion of low-frequency phonons in GaS (Ref. 40). The dashed lines correspond to a linear dispersion law.

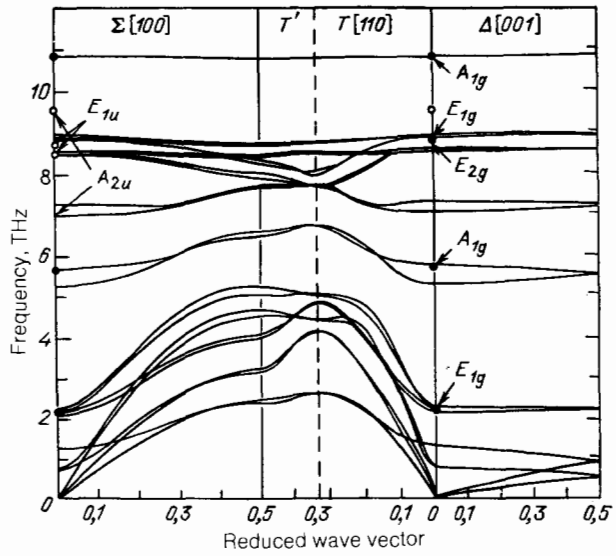

FIG. 7. Dispersion of phonons in GaS based on the data of Ref. 40 (complete picture).

the other hand, in the case of GaSe, PbI_2, and HgI_2 the dispersion law for the branch ω_3 is not quadratic. The above analysis is consistent with the experimental results. It is sufficient to examine Table II and compare the values of the elastic constants characterizing the interaction between atoms within the layers and between the layers in all these crystals.

The dispersion law is known to govern the density of states and the contribution of the various vibrations to the total density of phonon states. This circumstance gives rise to special features in the behavior of the thermal properties of strongly anisotropic crystals, which will be discussed in Sec. 3.

2.3. Optical phonons in layer crystals. Influence of pressure and temperature

The difference between the binding forces in layer crystals governs also the characteristics of optical vibrations. The general features of optical vibrations in layer crystals will be demonstrated by considering gallium sulfide as an example. Figure 7 shows the experimental results obtained by the method of slow neutron scattering in GaS (Ref. 40). The high-frequency optical vibrations lying in the range $\nu > 5$ THz correspond to displacements of atoms bound by strong ionic-covalent forces within the layers. Figure 7 demonstrates one other feature of the spectrum of optical phonons in layer crystals, which is the existence of low-frequency optical modes lying in the range $\nu \lesssim 1$ THz corresponding to displacements of layers relative to one another taken as a whole and regarded as rigid molecules. Low frequencies corresponding to interlayer vibrations have been found in the Raman scattering spectra of many layer crystals such as As_2S_3 (Refs. 41 and 42), MoS_2 (Ref. 43), GaSe (Ref. 44), GaS (Ref. 45), and InSe (Ref. 46).

The two-dimensional nature of the phonon spectrum of layer crystals is manifested by a weak dispersion of the high-frequency optical branches in the case of propagation of vibrations across the layers in crystals (along the Γ–Δ–A direction; see Fig. 7).

The existence of two types of binding in layer crystals is illustrated excellently in the experiments on the influence of hydrostatic pressures on the Raman spectra of layer crystals. Such experiments were carried out for GaS (Ref. 47), GaSe (Refs. 47 and 48), As_2S_3 (Ref. 49), InS (Ref. 50), and PbI_2 (Ref. 51). Figure 8 gives the results of an experimental study of the influence of hydrostatic pressures on the energy positions of the Raman scattering lines of GaS. A common feature of experiments of this kind, carried out at room temperature and pressures below 50 kbar, is that the low-frequency interlayer optical modes shift with pressure much faster than the high-frequency intralayer modes. The coefficient

$$\Gamma_\omega = \frac{1}{\omega}\frac{d\omega}{dp},$$

which represents shear, is an order of magnitude greater for the interlayer modes than for the intralayer modes. We note

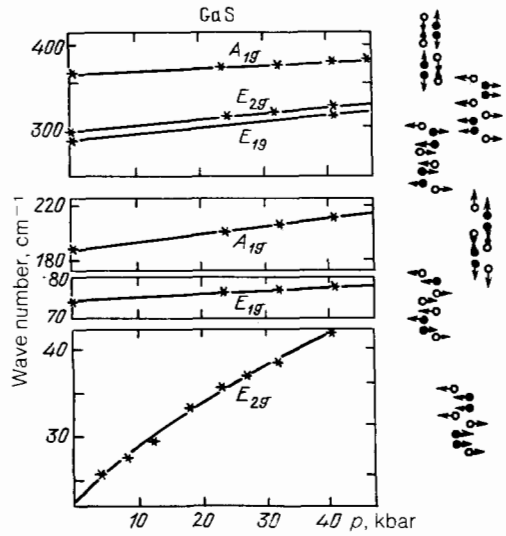

FIG. 8. Pressure dependences of the frequencies of Raman-active modes in GaS (Ref. 47). The displacement vectors are shown on the right.

that in comparing the values of the coefficient Γ_ω for monotypic modes in different layer crystals we have to allow for the different compressibilities of the crystals and in comparing the values of the same coefficient for different modes in the same crystal we have to allow for the difference between the compressibility of the crystal as a whole and that of a single layer.

The behavior of the compressibility of layer crystals, governed by changes in the elastic constants, determines the nonlinear pressure dependence of the parameter Γ_ω in the case of an interlayer low-frequency mode $\omega \approx 23$ cm^{-1} of GaS (see Fig. 8). An even more important factor is an allowance for the reduction in the compressibility on increase in the pressure when considering the results of the experiments carried out at high pressures in the range $p \lesssim 50$ kbar. The behavior of the spectrum of optical phonons in GaS under pressures up to 200 kbar at room temperature is described in Ref. 52. It is found that at pressures of ~ 150 kbar the $\omega \approx 23$ cm^{-1} low-frequency mode of GaS shifts to 76 cm^{-1}. It then follows from the model of the force constants that the values of these constants become equal for the interactions between the layers and within the layers. At 150 kbar the compound GaS exhibits three-dimensional properties in the sense considered here. The interlayer and intralayer optical vibrations in layer crystals also vary differently with temperature. Figure 9 shows the temperature dependences of the frequencies of two Raman-active modes in GaS. The mode ω_1 corresponds to an interlayer vibration (Fig. 8) and the mode ω_2 to an intralayer vibration. We can see that the relative changes in the frequency of the interlayer mode with temperature is faster than the change in the frequency of the intralayer mode. The fraction η of the total changes in the frequencies ω_1 and ω_2 due to the thermal expansion of a crystal, i.e., the fraction directly due to changes in the distances between the atoms, is estimated in Ref. 53. An analysis of the available data on the temperature dependences of the frequencies of optical phonons in other layer crystals, and also in molecular crystals,[54] allows us to draw the conclusion of the common nature of the temperature dependences of low-frequency interlayer or intermolecular vibrations and high-frequency intralayer or internal molecular vibrations: the contribution of the thermal expansion to the total change in the frequency of an interlayer or an intermolecular vibration is 70–80%, whereas in the case of intralayer or internal molecular vibrations the change in the frequency due to the thermal expansion is only 30–40%. Table IV gives the results of investigations of the temperature dependences of the frequencies of Raman-active vibrations in layer and molecular crystals. The contribution of the thermal expansion to the total temperature dependences of the frequencies can be found from the experimental results on the influence of hydrostatic pressures on the Raman scattering spectra of layer crystals. In estimating the thermal expansion contribution to the changes in the vibration frequencies with temperature we must use the results of measurements carried out on the same samples, as demonstrated by an analysis reported in Ref. 53. We can draw the conclusion that the temperature dependences of the frequencies of vibrations in layer and molecular crystals are monotypic, indicating a complex nature of the binding forces in layer and molecular crystals.

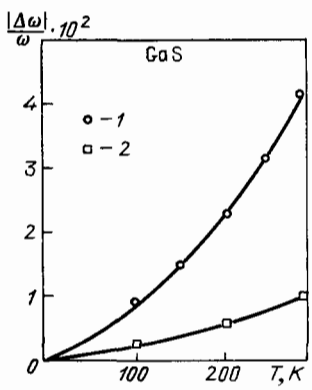

FIG. 9. Temperature dependences of the frequencies of Raman-active modes in GaS (Ref. 53): 1) $\omega = 23.2$ cm^{-1}; 2) $\omega = 190.1$ cm^{-1}.

TABLE IV. Contribution of thermal expansion to the temperature dependences of the frequencies of optical phonons in layer and molecular crystals.

Crystal	ω, cm^{-1}	η
GaSe, GaS [53]	20; 22, interlayer	0,75
	134; 188 intralayer	0,4
As_4S_4 [54]	39–65, intermolecular	0,78
	350, intramolecular	0,27
$C_{10}H_8$ [54]	46–125, intermolecular	1,5

We shall end this discussion of the characteristics of vibrational and elastic properties of layer crystals by noting that these features determine the unusual behavior of the physical phenomena observed in these crystals. One of these phenomena (thermal expansion) will be considered in the next section.

3. CHARACTERISTICS OF THERMAL EXPANSION OF LAYER CRYSTALS

3.1. Anisotropy of thermal expansion of graphite and boron nitride

We shall consider the changes which occur in the phonon spectra and elastic properties of layer crystals under pressure. In this section we shall use these results to describe the thermal expansion of anisotropic bodies.

The tensor of the linear thermal expansion of a crystal is described by[55]

$$\alpha_{ik} = \left(\frac{\partial u_{ik}}{\partial T}\right)_p. \tag{3.1}$$

We shall use the second law of thermodynamics in the form

$$dF = -s\,dT - u_{ik}\,d\sigma_{ik}; \tag{3.2}$$

here, F is the thermodynamic potential and s is the entropy, both per unit volume. The thermal expansion tensor is then

$$\alpha_{ik} = -\frac{\partial^2 F}{\partial\sigma_{ik}\,\partial T}. \tag{3.3}$$

The thermodynamic potential F can be written down by considering a solid as a set of noninteracting harmonic oscillators with frequencies ω_i.

Without allowance for the energy of the zero-point vibrations, we have

$$F=\frac{kT}{V}\sum_i \ln\left[1-\exp\left(-\frac{\hbar\omega_i}{kT}\right)\right]. \tag{3.4}$$

The principal values of the tensor α_{ik} for a crystal with axial symmetry become

$$\alpha_{zz}=-\frac{\partial}{\partial T}\left[\frac{1}{V}\sum_i \frac{\hbar\partial\omega_i/\partial\sigma}{\exp(\hbar\omega_i/kT)-1}\right],$$
$$\alpha_{xx}+\alpha_{yy}=-\frac{\partial}{\partial T}\left[\frac{1}{V}\sum_i \frac{\hbar\partial\omega_i/\partial p}{\exp(\hbar\omega_i/kT)-1}\right]; \tag{3.5}$$

here, $\sigma\equiv\sigma_{zz}$ and p is the stress created by hydrostatic pressure in a plane perpendicular to the symmetry axis.

The expressions in the system (3.5) are written down in what is known as the quasiharmonic approximation. In this approximation it is assumed that the frequencies of independent oscillators can vary with pressure.

In the case of a uniaxial crystal with the unit cell parameters a and c the derivatives of the frequencies with respect to the stress are

$$\frac{\partial\omega_i}{\partial\sigma}=\frac{\partial\omega_i}{\partial c}\frac{\partial c}{\partial\sigma}+\frac{\partial\omega_i}{\partial a}\frac{\partial a}{\partial\sigma},$$
$$\frac{\partial\omega_i}{\partial p}=\frac{\partial\omega_i}{\partial c}\frac{\partial c}{\partial p}+\frac{\partial\omega_i}{\partial a}\frac{\partial a}{\partial p}. \tag{3.6}$$

We shall substitute Eq. (3.6) into Eq. (3.5) and introduce Grüneisen parameters γ_{zz} and γ_{xx}. In contrast to Γ_ω (see Sec. 2.3), these parameters represent the relative changes in the frequencies in the case of elongations of a crystal along the symmetry (c) axis and at right-angles to this axis:

$$\gamma_{zz}=\frac{\sum_i \gamma_{zz,i}C_i}{\sum_i C_i}=-\frac{1}{C}\frac{\partial}{\partial T}\left[\sum_i \frac{\hbar\omega_i}{\exp(\hbar\omega_i/kT)-1}\frac{\partial\ln\omega_i}{\partial\ln c}\right],$$
$$\gamma_{xx}=\gamma_{yy}=\frac{\sum_i \gamma_{xx,i}C_i}{2\sum_i C_i} \tag{3.7}$$
$$=-\frac{1}{2C}\frac{\partial}{\partial T}\left[\sum_i \frac{\hbar\omega_i}{\exp(\hbar\omega_i/kT)-1}\frac{\partial\ln\omega_i}{\partial\ln a}\right];$$

here, $C=\sum C_i$ and C_i is the contribution of the ith mode to the specific heat.

The changes in the cell parameters with pressure described by $\partial c/\partial\sigma$, $\partial a/\partial\sigma$, $\partial c/\partial p$, and $\partial a/\partial p$ can be expressed in terms of the elastic constants if we use the theory of elasticity. The formulas for α_{ik} in a form convenient for analysis become:

$$\alpha_{zz}=\frac{C}{V}\left[\frac{C_{11}+C_{12}}{(C_{11}+C_{12})C_{33}-2C_{13}^2}\gamma_{zz}-\frac{2C_{13}}{(C_{11}+C_{12})C_{33}-2C_{13}^2}\gamma_{xx}\right],$$
$$\alpha_{xx}=\frac{C}{V}\left[\frac{C_{33}}{(C_{11}+C_{12})C_{33}-2C_{13}^2}\gamma_{xx}-\frac{C_{13}}{(C_{11}+C_{12})C_{33}-2C_{13}^2}\gamma_{zz}\right]. \tag{3.8}$$

In the case of a uniaxial layer crystal, we shall assume $\alpha_{xx}=\alpha_{yy}\equiv\alpha_\parallel$ (parallel to a layer in a crystal) and $\alpha_{zz}\equiv\alpha_\perp$ (perpendicular to a layer).

Studies of the thermal expansion are made by dilatometric methods. Changes in length are determined with the aid of a quartz dilatometer or x-ray diffraction methods, and also by laser interference dilatometry, capacitance methods, and some other techniques.[56,57]

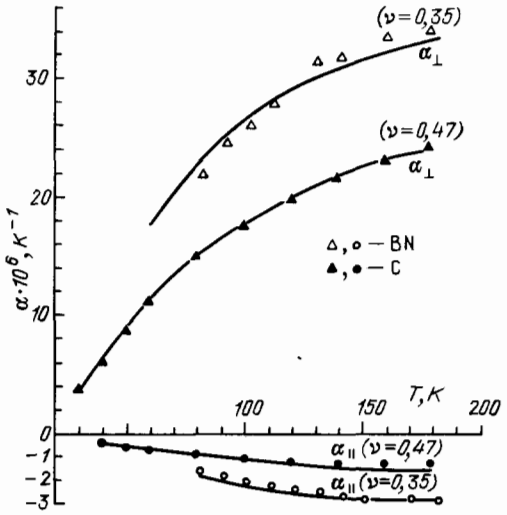

FIG. 10. Linear expansion coefficients of graphite[62] and boron nitride.[63] The continuous curves are calculated.[69,70]

The first detailed investigation of the temperature dependence of the thermal expansion coefficients of pyrolythic graphite was reported in Ref. 58. The x-ray diffraction method was used to determine the lattice parameters in a wide range of temperatures where $\alpha_\parallel$ was negative and a strong anisotropy of the linear expansion was observed. Subsequent experiments carried out by x-ray diffraction[59–61] and interferometric[62] methods confirmed that $\alpha_\parallel$ was negative in the temperature range 20–650 K. It was also found that in the case of boron nitride[63] the corresponding range of temperatures was even wider extending up to 850 K.

The negative linear expansion of layers in graphite is typical of materials prepared by different methods[64] and also of its intercalated compounds.[65] Figure 10 gives the temperature dependences of the linear expansion coefficients of graphite and boron nitride. The temperature dependences of these coefficients can be analyzed quantitatively on the basis of the expressions in Eq. (3.8) provided we know the dispersion laws of the branches and the behavior of the relevant frequencies under pressure; we also need the specific heat data. We shall now consider the possible origin of the negative thermal expansion of anisotropic crystals using the expressions in Eq. (3.8) and following the treatments in Refs. 66 and 67. The negative value of $\alpha_\parallel$ for graphite is related to the dominant role of the second term in the expressions in Eq. (3.8). It is in fact assumed that the lateral compression due to strong expansion at right-angles to the layers is much greater than the expansion of the layers due to increase in temperature. In view of the strong anisotropy such that C_{33}, $(C_{11}+C_{12})\gg 2C_{13}^2$, it follows from the last conclusion that the system (3.8) can be represented in the form

$$\alpha_\perp\approx\frac{C}{V}\gamma_{zz}\frac{1}{C_{33}},$$
$$\alpha_\parallel\approx-\frac{C}{V}\gamma_{zz}\frac{C_{13}}{(C_{11}+C_{12})C_{33}}. \tag{3.9}$$

Hence we find that

$$\frac{|\alpha_{\parallel}|}{\alpha_{\perp}} \approx \frac{C_{13}}{C_{11}+C_{12}}. \qquad (3.10)$$

The ratio on the right-hand side of Eq. (3.10) is the Poisson ratio for a crystal of hexagonal synmetry which represents the change in the dimensions of this crystal in the plane of its layers on application of a pressure along the symmetry axis. At room temperature, graphite is characterized by $|\alpha_{\perp\parallel}|/\alpha_{\perp} = 0.04$ and $C_{13}/(C_{11}+C_{12}) = 0.01$. The lateral compression due to expansion of the crystal along the c axis plays a very small role.

It therefore follows that the existence of a wide range of temperatures in which a graphite crystal is compressed as a result of heating cannot be explained by the Poisson compression. It is necessary to assume that γ_{xx} is negative. This means that heating tends to minimize the total energy of a crystal by reducing the frequencies of the vibrations and this reduction is not due to an increase in the dimensions of a crystal, as is true in most cases, but due to a reduction in these dimensions. Before considering this case in greater detail, we shall first discuss the published data on the thermal expansion of layer semiconductors.

3.2. Thermal expansion of layer semiconductors

In spite of the fact that many layer semiconductors are known at present, the thermal expansion coefficients have been determined in a wide range of temperatures only for a few crystals. The fullest investigations of the dependences $\alpha_{\parallel}(T)$ and $\alpha_{\perp}(T)$ have been made for III–VI semiconductor compounds. A quartz dilatometer was first used in Ref. 68 to study the thermal expansion of large samples of GaSe, GaS, and InSe with dimensions up to 30 mm. Similar investigations of samples with dimensions up to 5 mm were carried out by interferometric methods.[69,70] Figure 11 shows the temperature dependences of $\alpha_{\parallel}$ and $\alpha_{\perp}$ plotted for gallium sulfide on the basis of the data reported in Refs. 68 and 69. The curves obtained in Refs. 69 and 70 demonstrate a strong anisotropy of the thermal expansion and negative values of $\alpha_{\parallel}$ in the temperature range 30–50 K, whereas the results reported in Ref. 68 suggest a weak anisotropy; the coefficient $\alpha_{\parallel}$ is positive. A weak anisotropy of the linear expansion suggests that the large samples used in Ref. 68 are characterized by misorientation of the layers and by stacking defects. Figure 12 gives the results obtained for gallium and indium selenides, which are again characterized by an anisotropy of α and negative values of $\alpha_{\parallel}$ in the range 30–50 K.

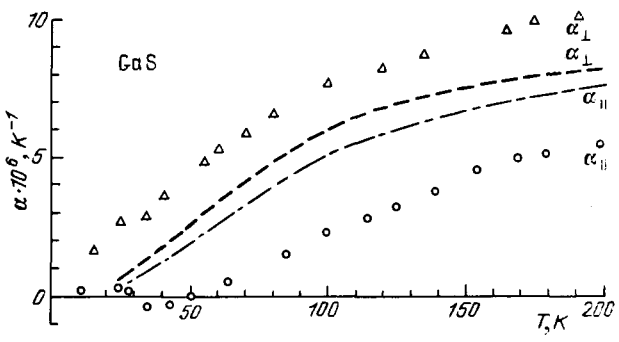

FIG 11. Linear expansion coefficients of GaS (Ref. 69). The dashed and chain curves are taken from Ref. 68.

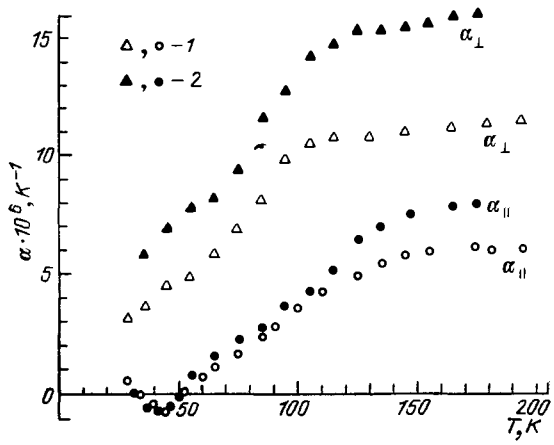

FIG. 12. Thermal expansion coefficients of GaS (1) and InSe (2), taken from Refs. 69 and 70.

The published data on the thermal expansion of cadmium iodide[71] (Fig. 13) are characterized by a monotonic temperature dependence and positive values of $\alpha_{\parallel}$ and $\alpha_{\perp}$.

The temperature dependences of the thermal expansion coefficients of ternary crystals $TlInS_2$ and $TlGaS_2$ are plotted in Fig. 14 (on the basis of the data taken from Refs. 69 and 72). In the case of these crystals we find that $\alpha_{\parallel} > 0$ and the anomaly of $\alpha_{\perp}$ observed for $TlInS_2$ at 200 K is attributed to structural phase transitions.

The phase transitions associated with a charge-density wave affect the temperature dependences of the thermal expansion coefficients of $TaSe_2$-type semiconductors.[73,74] We shall not discuss the nature of the thermal expansion of these crystals. As far as the other experiments are concerned it is worth noting the following. The thermal expansion anisotropy is typical of crystals which have a strong anisotropy of the elastic constants. The region of negative thermal expansion is typical of crystals whose elastic properties are strongly anisotropic.

In the next subsection we shall discuss the nature of the temperature dependences of the linear expansion coefficients of graphite and III-VI layer semiconductor compounds using a theory of thermal properties of strongly anisotropic crystals.

3.3. Nature of negative thermal expansion of layer crystals. Lifshitz membrane effect

We shall calculate the linear expansion coefficients of a strongly anisotropic crystal starting with the dispersion laws for acoustic waves of Eq. (2.9) in the form suggested by I. M.

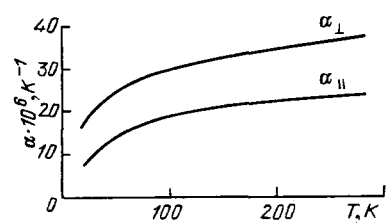

FIG. 13. Thermal expansion coefficients of CdI_2 (Ref. 71).

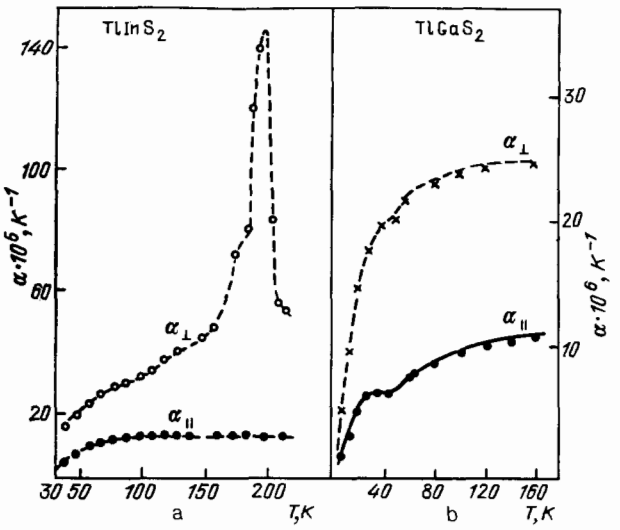

FIG. 14. Thermal expansion coefficients of $TlInS_2$ (a, Ref. 69) and $TlGaS_2$ (b, Ref. 62).

Lifshitz:

$$\begin{aligned}\omega_1^2 &= c_1^2(k_x^2+k_y^2)+c^2\eta^2k_z^2,\\ \omega_2^2 &= c_2^2(k_x^2+k_y^2)+c^2\eta^2k_z^2,\\ \omega_3^2 &= c^2\eta^2(k_x^2+k_y^2)+c^2\xi^2k_z^2+\gamma^2(k_x^2+k_y^2)^2;\end{aligned} \tag{3.11}$$

in Eq. (3.11), we have

$$c_1^2=\frac{C_{11}-C_{12}}{2\rho},\quad c_2^2=\frac{C_{11}}{\rho},\quad c^2=\frac{2c_1^2c_2^2}{c_1^2+c_2^2},$$
$$\eta^2=\frac{C_{44}}{\rho c^2},\quad \xi^2=\frac{C_{33}}{\rho c^2},$$

where ξ and η are small parameters in view of the strong anisotropy of the elastic properties. The value of γ representing the flexural rigidity is estimated in Ref. 2 on the assumption that the limiting frequencies of flexural vibrations cannot exceed the highest frequencies in the acoustic spectrum:

$$\gamma\left(\frac{\pi}{a}\right)^2=\nu c\frac{\pi}{a},\quad \gamma=\frac{cav}{\pi}; \tag{3.12}$$

here, π/a is the maximum value of the wave vector and ν is a fitting parameter smaller than unity. Using the elastic constants of graphite (Table II) we can describe the experimental results plotted in Fig. 5 by selecting $\nu = 0.47$.

It follows from the dispersion laws of Eq. (3.11) that flexural vibrations correspond to the maximum density of states and that they make the dominant contribution to the thermal properties at sufficiently low temperatures. For example, when the values of k_x and k_y are low, so that the term $\sim(k_x^2+k_y^2)^2$ can be ignored, the function describing the density of states is

$$g(\omega)=\frac{\omega^2}{2\pi^2}\left(\frac{1}{c_1^2c\eta}+\frac{1}{c_2^2c\eta}+\frac{1}{c^3\eta^2\xi}\right). \tag{3.13}$$

In view of the smallness of η and ξ, the highest density of states corresponds to the flexural branch. This is an important point in the discussion of the thermal properties of strongly anisotropic crystals.

We shall now calculate the thermal expansion coefficients. The expression (3.5) for the components of the thermal expansion tensor will be rewritten integrating with respect to the wave vector inside the Brillouin zone and including only the contribution of the flexural branch:

$$\begin{aligned}\alpha_\perp &= -\frac{1}{(2\pi)^3}\frac{\partial}{\partial T}\int\limits_{-k_m}^{+k_m}\int\int\frac{\hbar\partial\omega_3^2/\partial\sigma}{2\omega_3\left[\exp\left(\hbar\omega_3/kT\right)-1\right]}\,d^3\mathbf{k},\\ \alpha_\parallel &= -\frac{1}{2}\frac{1}{(2\pi)^3}\frac{\partial}{\partial T}\int\limits_{-k_m}^{+k_m}\int\int\frac{\hbar\partial\omega_3^2/\partial p}{2\omega_3\left[\exp\left(\hbar\omega_3/kT\right)-1\right]}\,d^3\mathbf{k}.\end{aligned} \tag{3.14}$$

Using the dispersion law of Eq. (3.11), we find that the expression for $\alpha_\perp$ can be reduced to

$$\alpha_\perp=-\frac{1}{(2\pi)^3}\frac{\partial}{\partial T}\int\limits_{-k_m}^{+k_m}\int\int\frac{\hbar\left[(k_x^2+k_y^2)\frac{\partial C_{44}}{\partial\sigma}+k_z^2\frac{\partial C_{33}}{\partial\sigma}+(k_x^2+k_y^2)^2\frac{\partial(\rho\gamma^2)}{\partial\sigma}\right]}{2\rho\omega_3(\mathbf{k})\left[\exp\left(\hbar\omega_3(\mathbf{k})/kT\right)-1\right]}\,d^3\mathbf{k}. \tag{3.15}$$

In the calculations we need to know not only the elastic constants, but also their pressure derivatives. We need to know the influence of uniaxial pressure on the elastic constants C_{44}, C_{33}, C_{11}, and C_{12}. The values of the constants C_{11}, C_{12}, C_{13}, and C_{44} for graphite are given in Table II, but there are practically no data on the influence of uniaxial pressures on the values of the components of the elasticity tensor. We shall use Table III which is a collection of the results of experimental studies of the influence of hydrostatic pressures on the elastic constants of layer crystals. We are justified in using the data on hydrostatic compression because in the crystals with a weak binding between the layers a reduction in the interatomic distance as a result of compression along the c axis is the same as under hydrostatic pressure. It follows from Tables II and III that $\partial C_{44}/\partial\sigma \ll \partial C_{33}/\partial\sigma$. Moreover, in view of the weak binding between the layers, the reduction in the interlayer distances under pressures $p\|c$ has little influence on the "interlayer" elastic constants. The inequalities $\partial C_{11}/\partial\sigma$, $\partial C_{12}/\partial\sigma \ll \partial C_{33}/\partial\sigma$ can be assumed to be satisfied. Using these inequalities in the calculation of $\alpha_\perp$, we need retain only the second term in the numerator of Eq. (3.15) and thus reduce the nunber of fitting parameters to two: $\partial C_{33}/\partial\sigma$ and ν. Selecting $\nu = 0.47$ and $\partial C_{33}/\partial\sigma = -16.5$, we can describe satisfactorily the experimental data for graphite reported in Refs. 70 and 75 (Fig. 10). As pointed out already, $\nu = 0.47$ is in agreement with the dispersion laws of acoustic waves in graphite and $\partial C_{33}/\partial\sigma = -16.5$ agrees well with the experimental data given in Tables II and III (the minus sign corresponds to an increase in C_{33} under pressure).

It is appropriate to mention that calculations indicate that in the temperature range up to 200 K a change in the elastic constant C_{44} within the range 0.04×10^{11} dyn/cm^2 $\leqslant C_{44} \leqslant 0.2\times10^{11}$ dyn/cm^2 has little effect on $\alpha_\perp$: this quanti-

ty changes by just a few percent. This is because in the investigated temperature range we can ignore the term $\left(\frac{C_{44}}{\rho}\right)(k_x^2 + k_y^2)$ in the dispersion law for flexural waves.

The temperature dependence $\alpha_\perp(T)$ for boron nitride can also be described satisfactorily using the elastic parameters of graphite and assuming that $\nu = 0.35$, in accordance with Refs. 70, 75, and 76 (Fig. 10).

The situation is somewhat different in the case of calculations of $\alpha_\parallel$ for graphite and boron nitride. It is reported in Refs. 70 and 75 that the concept of the "membrane effect" has to be used in the calculation of $\alpha_\parallel(T)$ for graphite and boron nitride. This concept was first put forward by I. M. Lifshitz[2] in 1952. This effect is manifested in the thermal expansion as follows: flexural acoustic waves, excited in a layer crystal at temperatures such that these waves dominate the thermal properties, reduce the dimensions of the crystal along the layers but do not affect the distances between the neighboring atoms in a layer, so that $\alpha_\parallel = 0$.

It follows from Eq. (3.14) that the sign of $\alpha_\parallel$ is governed by the sign of the derivative $\partial\omega_i/\partial p$. As pointed out already, the contribution of flexural waves dominates the thermal properties at low temperatures and the sign of the derivative determines $\partial\omega_3/\partial p$.

When a pressure stretching the layers is applied to a crystal, the layers resemble membranes, i.e., thin stretched plates. In a membrane (or in a stretched string) the forces due to the displacements of atoms at right-angles to the membrane are governed primarily by the longitudinal elongation.[34,35] The frequencies of transverse vibrations in a membrane (string) are proportional to the square root of the restoring force.

In the case of a membrane the dispersion law for flexural vibrations is of the form

$$\omega^2 \approx \frac{p}{\rho}\varkappa^2;$$

here, $p = F/l$, F is an omnidirectional stretching force, l is the perimeter of a membrane, and $\varkappa^2 = k_x^2 + k_y^2$. This makes it possible to write down the dispersion law for the flexural branch in the form[2]

$$\omega_3^2 = c^2\eta^2\varkappa^2 + c^2\xi^2 k_z^2 + \gamma^2\varkappa^4 + \frac{p}{\rho}\varkappa^2. \tag{3.16}$$

We shall now calculate the derivative $\partial\omega_3/\partial p$ for a stretched layer:

$$\frac{\partial\omega_3}{\partial p} = \frac{1}{2\omega_3}\left[\varkappa^2\frac{\partial(c^2\eta^2)}{\partial p} + k_z^2\frac{\partial(c^2\xi^2)}{\partial p} + \varkappa^4\frac{\partial\gamma^2}{\partial p} + \varkappa^2\frac{1}{\rho}\right]. \tag{3.17}$$

The first two terms in Eq. (3.17) can be ignored because the change in the interlayer constants is small when a layer is extended. Then, if $\gamma^2 = c^2a^2\nu^2/\pi^2$, the derivative $\partial\omega_3/\partial p$ becomes

$$\frac{\partial\omega_3}{\partial p} = \frac{\varkappa^2}{2\rho\omega_3}\left[1 + \frac{\nu^2}{\pi^2}(a\varkappa)^2\frac{\partial(\rho c^2)}{\partial p}\right]. \tag{3.18}$$

The value of $\partial(\rho c^2)/\partial p$ is governed by the pressure dependences of the interlayer constants and is of the order of 10. Bearing in mind that in the long-wavelength appoximation we have $a\varkappa \ll 1$ and $\nu < 1$, we can write down

$$\frac{\partial\omega_3}{\partial p} \approx \frac{\varkappa^2}{2\rho\omega_3} > 0. \tag{3.19}$$

The increase in the frequencies of "flexural" vibrations due to elongation was called by I. M. Lifshitz the membrane effect.

Since $\partial\omega_3/\partial p$ is positive, the coefficient $\alpha_\parallel$ will have the negative sign. Using the expression in Eq. (3.19) to calculate $\alpha_\parallel(T)$ and assuming the values of $\nu = 0.47$ for graphite and $\nu = 0.35$ for boron nitride, we can describe satisfactorily the available experimental data (Fig. 10). Therefore, the characteristic features of the thermal expansion of graphite and boron nitride are due to the existence of "flexural" waves typical of the acoustic spectrum of a strongly anisotropic crystal. These flexural waves give rise to a negative linear expansion in the plane of the layers because of the membrane effect.

We shall consider now the role of the membrane effect in the thermal expansion of other layer crystals. We shall discuss particularly the most thoroughly investigated group of semiconductors with the gallium selenide structure. The dependences $\alpha_\parallel(T)$ and $\alpha_\perp(T)$ are plotted in Figs. 11 and 12. The temperature dependences of $\alpha_\perp$ and $\alpha_\parallel$ obtained for GaSe, GaS, and InSe have the following common features: the dependence $\alpha_\parallel(T)$ passes through a range of negative values of $\alpha_\parallel$ at temperatures 30–50 K; above 50 K the values of $\alpha_\parallel$ become positive for all the crystals and they cease to depend on temperature in the range $T \geqslant 150$ K.

The nature of the negative thermal expansion of III–VI binary layer semiconductors will be discussed following Ref. 75 and considering gallium sulfide as an example because of the strongest anisotropy of its elastic constants compared with the series of its structural analogs (Table II). The acoustic spectrum of gallium sulfide exhibits the same features as the spectrum of graphite (see Figs. 5 and 6).[17] The anisotropy of the elastic constants of GaS, GaSe, and InSe is not demonstrated as strikingly as that of graphite (Table II). The interaction between layers in graphite is much stronger. In the calculations of the thermal expansion we can no longer ignore the contribution of the branches ω_1 and ω_2. This can be easily demonstrated using the expression for the density of states given by Eq. (3.13). An analysis of the nature of the thermal expansion of gallium sulfide and its analogs requires an allowance for the branches ω_1 and ω_2. The necessary calculations were carried out in Ref. 75 using the data of Table II and assuming the values $\nu = 0.6$ and $\partial C_{11}/\partial p = -16$. Figure 15 demonstrates satisfactory agreement between these numerical calculations and experiments.

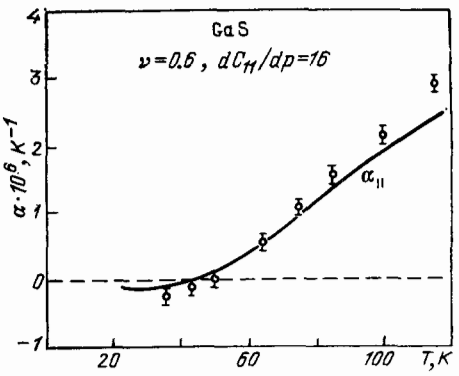

FIG. 15. Temperature dependence of $\alpha_\parallel$ for GaS (Ref. 69). The continuous curve is calculated.

Clearly, the existence in a narrow temperature range of negative values of the linear thermal expansion coefficients α_1 of gallium sulfide and its analogs can be attributed to the membrane effect. On further increase in temperature the contribution of the modes ω_1 and ω_2 associated with the intralayer vibrations of atoms increases and the values of $\alpha_\parallel$ become positive. The positive contribution of the branches ω_1 and ω_2 is due to the sign of the derivative $\partial\omega_{1(2)}/\partial p$ and the elastic intralayer constants decrease on elongation of a crystal. It is clear from this discussion that in the case of layer crystals exhibiting an anisotropy even weaker than that of gallium sulfide the range of negative values of $\alpha_\parallel$ may not be observed (this is true, for example, of PbI_2 and its analogs). The negative linear expansion due to the membrane effect may not be observed either in strongly anisotropic crystals if for some reason the flexural rigidity of the layers is high. In this case the flexural waves are excited at fairly high temperatures when the role of optical vibrations is important. Such a situation may occur in ternary semiconductors of the $TlGaS_2$ type. Finally, we note that the membrane effect can occur in any strongly anisotropic crystal and it can either give rise to negative values of $\alpha_\parallel$ or it can reduce the values of the relevant tensor components. From this point of view we have to analyze the experimental data on the thermal expansion of tellurium, zinc,[77,78] etc.

4. INFLUENCE OF PRESSURE ON THE BAND STRUCTURE OF LAYER SEMICONDUCTORS

4.1. Band structure of layer semiconductors

The band structure has been calculated so far for a limited number of layer semiconductors. The most detailed calculations have been carried out by the empirical pseudopotential method for III–VI semiconductor crystals.[79–81] Recently new data have been reported on the band structure of IV–VI layer crystals.[82] The first calculations of the band structure of GaSe carried out in the two-dimensional approximation about 20 years ago[83–89] describe correctly the order of states in the valence band and the energy gaps between the band extrema. However, a complete picture of the optical transitions and their polarization features, as well as the distribution of the electron density in layer crystals were obtained by considering the real three-dimensional crystal structure of gallium selenide.[79] This analysis was applied to β-GaSe with the space symmetry group D_{6h}^4 (Fig. 16). According to this scheme, the top of the valence band at $K = 0$ is the state Γ_4^-. The conduction band has two minima: at the center of the Brillouin zone Γ_3^+ and at the edge of the zone M_3^+. Further experiments[85] demonstrated that the energies of these minima differ only very slightly. Direct and indirect transitions are allowed when the electric vector has the $\mathbf{E}\|c$ orientation. The $\mathbf{E}\|c$ transitions are allowed as a result of interband mixing of the Γ_4^- and $\Gamma_{5,6}^+$ states due to the spin-orbit interaction.

An important feature is the three-dimensional nature of direct excitons in gallium selenide. Experimental investigations[85–87] demonstrated that the exciton series of GaSe is described well by the three-dimensional dependence

$$E_n = -Rn^{-2} \qquad (n = 1, 2, 3),$$

and not by the two-dimensional dependence

$$E_n = -R\left(n + \frac{1}{2}\right)^{-2} \qquad (n = 0, 1, 2, 3).$$

The anisotropy of the effective masses of electrons and holes in gallium selenide $m_\parallel/m_\perp$ (the symbol $\parallel$ denotes the orientation along the layers and $\perp$ is the orientation across the layers) is weak.[1] The energy band structure of indium selenide is the same as the band structure of GaSe described above, except for the difference between the band gaps: in the case of gallium selenide at 4.2 K we have the direct band gap $E_g^d = 2.132$ eV, whereas the corresponding value for InSe is $E_g^d = 1.36$ eV (Refs. 88–90).

Gallium sulfide has a wider band gap: the indirect gap is $E_g^i = 2.36$ eV and the direct one is $E_g^d = 3.08$ eV (Ref. 91). Nevertheless, the general pattern of the optical transitions in all crystals is very similar. A distinguishing feature of the energy band scheme for all three crystals is the presence of bands of two types for which the wave functions: 1) are concentrated mainly around and between the atoms of a metal within a single layer; 2) include p_z orbitals located at the boundaries of the neighboring layers of Se atoms, so that they are concentrated in the space between layers.

States of the first type are of small "width" in the direction along k_z of the hexagonal Brillouin zone; such states form two-dimensional bands which, according to theoretical calculations, are the valence bands ($\Gamma_{5,6}^{+\,-}$). However, the

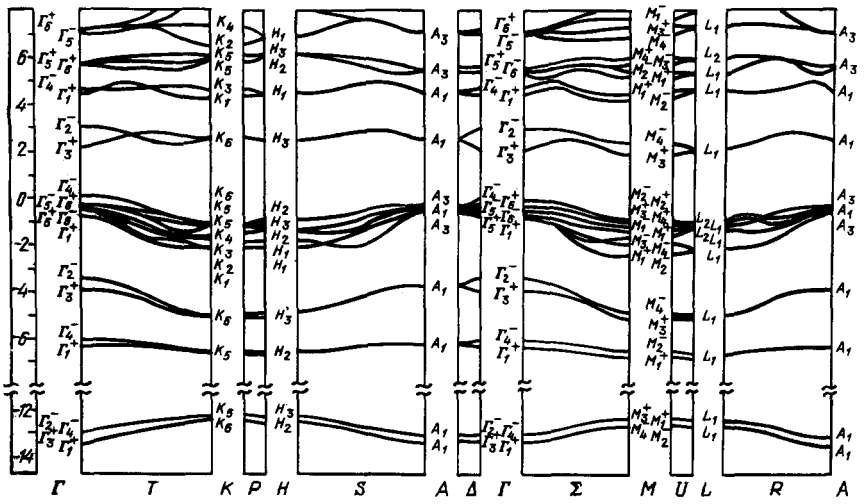

FIG. 16. Energy band structure of β-GaSe (Ref. 79).

highest valence band and the lowest conduction band at $K = 0$ for GaS, GaSe, and InSe are three-dimensional because their formation includes a significant participation of the p_z orbitals of selenium or sulfur. The existence of two- and three-dimensional bands of layer crystals, like the validity of the calculations of Ref. 79, has been demonstrated employing the highly popular method of photoemission with angular resolution.[92-95]

The highest group of the valence bands $\Gamma_4^- \Gamma_1^+$, the optical transitions to which form the absorption edge of GaSe and InSe, exhibit a strong (~ 1 eV) dispersion along the direction perpendicular to the layers in a crystal. These three-dimensional states are characterized[79] by a considerable contribution of the p_z orbitals of selenium to the corresponding electron density. The group of two-dimensional bands Γ_5^+, Γ_5^-, Γ_6^+, and Γ_6^- is characterized by a weak dispersion along k_z (~ 0.3 eV). These states manifest mainly the $p_{x,y}$ nature (Fig. 16). The degree of mixing of p_z-like charges localized near Se atoms determines the different degrees of dispersion of the deeper states Γ_2^-, Γ_3^+ and Γ_1^+, Γ_4^-.

We shall use the example of gallium selenide and its analogs to demonstrate that the electron states in layer crystals can be two- or three-dimensional. The existence of isotropic electron states is due to an overlap between the individual layers of the p_z orbitals of the anions, which make the main contribution to the corresponding electron density. The degree of such overlap determines the values of the elastic constants characterizing interlayer vibrations (see Ref. 1). On the other hand, the orbitals of the metal and the $p_{x,y}$ orbitals of the chalcogens, which show little overlap between the individual layers, form an electron density corresponding to strongly anisotropic and two-dimensional states; the magnitude and distribution of the electron charge density, concentrated between the individual atoms in a layer characterize the higher frequencies of intralayer phonon modes.

Another important feature of the electron spectra of layer crystals is the circumstance that in a crystal with a unit cell consisting of two layers the states are linked in pairs and the interlayer interaction results in the splitting of the bands into pairs. In the scheme shown in Fig. 16 the bands have different parities relative to the inversion operation (for example, Γ_4^- and Γ_1^+; Γ_3^+ and Γ_2^-, etc.). The pair nature of the states is characteristic of the electronic spectra and also of other layer semiconductors such as GeSe and its analogs.[82]

The existence of two types of states and the splitting of the bands by the interlayer interaction in the electron structure is attracting interest to the influence of pressure (both hydrostatic and uniaxial) on various properties of layer crystals. The application of a pressure alters the distances between the layers and thus modifies the interlayer interaction and makes it possible to find to what extent this interaction determines the nature of the electron spectrum of any particular layer semiconductor. In the next subsections we shall consider the influence of pressure on optical properties of some layer semiconductors.

4.2. Influence of hydrostatic pressure on optical spectra of layer semiconductors

We shall consider the results of experimental investigations of hydrostatic pressure on the exciton spectra of GaSe-type semiconductors, the band structure of which we discussed in considerable detail in the preceding subsection. These experiments were carried out mainly by two teams of physicists[96-103] using similar experimental methods. Thin (~ 10–$16\ \mu$m) crystals of gallium selenide and sulfide split off from massive blocks were placed in a high-pressure chamber which had sapphire windows; a methanol-ethanol mixture or a polysiloxane liquid was used as the pressure-transmitting medium (helium was employed at low temperatures of the order of 77 K). Pressures were measured using pressure sensors or the shift of the emission line of a standard subjected to laser excitation.

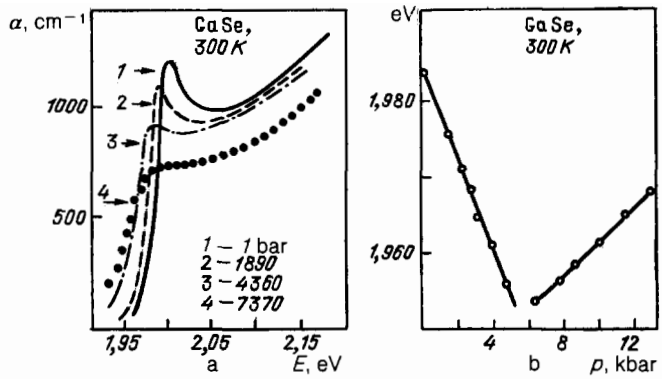

FIG. 17. a) Exciton absorption spectra of GaSe recorded at different hydrostatic pressures.[98] b) Pressure dependence of the exciton energy E (Ref. 98).

Figure 17a shows the absorption spectra of GaSe recorded in the range of energies of direct exciton transitions under various pressures applied at room temperature. Figure 18a gives the corresponding dependences for GaS and in this case the experiments were carried out at 77 K.

Figures 17a and 18a demonstrate clearly the change in the absorption coefficient at the maximum of an exciton peak of GaSe and GaS.

The reason for this behavior is clearly associated with a

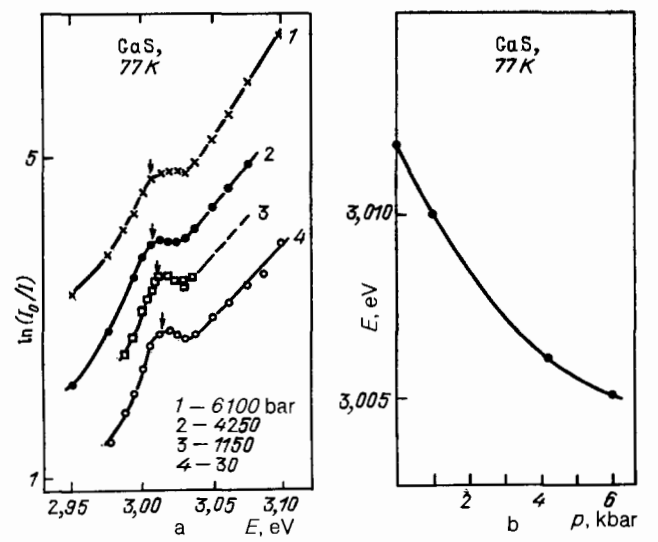

FIG. 18. a) Exciton absorption spectra of GaS recorded at different hydrostatic pressures.[102] b) Pressure dependence of the exciton state energy.[102]

change (under the applied pressure) in the interband mixing of the Γ_4^- band (of p_z nature) with a group of two dimensional bands $\Gamma_{5,6}^{(\pm)}$ (of $p_{x,y}$ nature). The different anisotropies of these bands and the different symmetries are responsible for the difference between the corresponding deformation potentials.

We observe clearly a shift of the energy position of the maximum of the exciton peak toward longer wavelengths (Figs 17b and 18b). The energy shift recorded in experiments of this kind was due to a pressure-induced change in the band gap and not due to a change in the exciton binding energy. In fact, since the binding energy was determined primarily by the permittivity and the effective mass, a small change in these parameters had practically no effect on the exciton binding energy.

A reduction in the band gap under pressure can be explained using the energy band structure shown in Fig. 16. As pointed out already, one of the characteristics of the energy band structure of GaSe-type layer crystals is the pair nature of the bands due to the interlayer interaction. In the case of β-GaSe and GaS a unit cell is formed from two layers in such a way that the layers can be made to coincide by applying the inversion operation. This means that each energy state in an isolated layer splits into two in a crystal (in the case of molecular crystals this is known as the Davydov splitting or the factor group splitting[104]). Enhancement of the interaction between layers, such as that due to the application of pressure, can increase the splitting. The conduction bands of GaSe and GaS (Γ point) represent the lower component of the doublet Γ_3^+ and Γ_2^-, whereas the valence band represents the upper component of the doublet Γ_4^- and Γ_1^+. Figure 19 shows the origin of the long -wavelength shift of the exciton transitions characterized by $K = 0$ and occurring in GaSe and GaS under pressure.

This approach is clearly valid in a study of the pressure dependences of the properties of a series of layer semiconductors with the band gaps which decrease under pressure: HfS_2, $HfSe_2$, SnS_2, and $SnSe_2$ (Refs. 105–108). A characteristic feature is that for the majority of these crystals the results of calculations of the energy band structure demonstrate, as in the case of GaSe, that at least one of the states at the absorption edge has an electron density formed with the participation of the p_z orbitals of the atoms located at the boundaries of the layers. In the case of HfS_2 the top of the

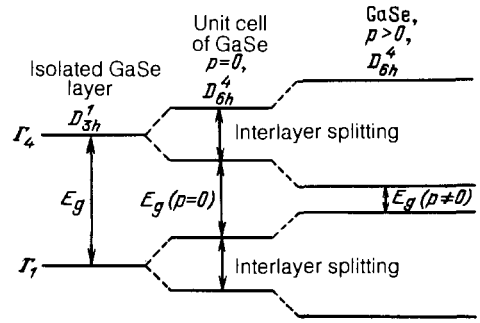

FIG. 19. Band shifts in a layer crystal under pressure: 1) $p = 0$; 2) $p \| c$; 3) $p \perp c$.

valence band is formed in the presence of a considerable admixture of the p_z orbitals of sulfur, whereas in the case of SnS_2 and $SnSe_2$ both the conduction and the valence bands include the p_z orbitals of S and Se (Refs. 109 and 110). In this case the change in the interlayer distance shifts considerably (along the energy scale) the bands the electron densities of which are located between the layers.

This general approach to the pressure coefficients of a number of layer crystals is naturally not universal. In the case of semiconductors with the absorption edge characterized by electron states of different origin than in the case of GaSe the magnitudes and signs of the pressure coefficients $\partial E_g/\partial p$ can vary greatly. Typical examples are crystals of PbI_2, CdI_2, and MoS_3 and several others. In the case of these crystals the main contribution to the states at the absorption edge is made by metal atoms located within the layers.[109,111,112] The pressure coefficients of the direct energy gaps $\partial E_g^d/\partial p$ of crystals subjected to hydrostatic pressures at 300 K are positive for CdI_2 and MoS_2 and negative for PbI_2 (Refs. 105 and 113–115).

It follows from the data in Table V that in the case of GaSe (GaS) and $SnSe_2$ (SnS_2) the negative pressure coefficients are typical of indirect transitions. The sign of $\partial E_g^i/\partial p$ is not surprising, but the values of $\partial E_g^d/\partial p$ larger than $\partial E_g^i/\partial p$ are difficult to explain on the basis of the band structure of these semiconductors.

Some difficulties are also encountered in the explanation of the special nature of the influence of the pressure coefficients of the band gaps of GaSe and GaS. Figures 17b

TABLE V. Pressure coefficients of the band gaps of layer crystals (10^{-6} eV/bar).

Crystal	T, K	P	E_g^d	E_g^i	Ref.
HfS_2	300	hydrostatic	−7	—	105
$HfSe_2$	ditto	»	−9,6	—	105
SnS_2	» »	»	−2	−11,5	106
$SnSe_2$	» »	»	−4,5	−10,5	106
GaS	77	»	−2	−12	102
	5	$p \| c$	+4	−2	117, 118, 120
	5	$p \perp c$	—	−5	118
GaSe	300	hydrostatic	−4	−11,5	98, 100, 103
	5	$p \| c$	+2	—	117
	5,300	$p \perp c$	−10	—	116, 118
InSe	300	hydrostatic	−3,5	—	51
GeS	ditto	»	−5	—	108
SnSe	» »	»	−6,5	—	107
MoS_2	» »	»	+1,4	—	105
PbI_2	» »	»	−17,5	—	113
CdI_2	» »	»	+2	—	114

and 18b show the pressure dependences of the shift of the energy of the exciton absorption maximum (at $K = 0$) obtained for GaSe and GaS in Refs. 98 and 102, respectively. We can easily see the effect of a change in the sign of the pressure coefficient $\partial E_g^d/\partial p$ in the case of GaSe and a strong dependence of $\partial E_g^d/\partial p$ on the pressure applied to GaS.

In discussing the results of these experimental investigations carried out under hydrostatic pressure it is difficult to identify the reason for the dependence of $\partial E_g^d/\partial p$ on the pressure applied to layer crystals. We shall return to this topic after reporting the experimental results of a study of uniaxial deformation of GaSe and GaS. We shall conclude this subsection by noting that little work has been done on the problem of structure phase transitions which can occur in weakly bound crystals under pressure. Apparently, there can be two transitions of this type: transitions from one polytype to another and structural transitions within one polytype.[89] Since the energies corresponding to the band widths differ by several tens of meV for different polytypes, phase transitions can be used to explain various anomalies of the pressure dependences of the energy positions of the absorption peaks, interference maxima in the transparency band, and temperature coefficients of the band shifts.

4.3. Influence of uniaxial deformation on optical properties of layer semiconductors

The special nature of the crystal structure of layer materials makes it difficult to carry out investigations of their properties under uniaxial deformation conditions. First of all, it is difficult to ensure the reversible nature of the applied perturbation. In the case of optical experiments the working face of a crystal is frequently a cleavage plane perpendicular to the c axis. Therefore, in the case of deformation along the c axis it is desirable to direct a light flux and the stress along the same direction. In an investigation of the influence of elongation of thin plates ($< 100\,\mu$m) on their optical properties there is a danger that the layers may be ruptured and exhibit plastic flow. This is the reason for the few experimental results on the influence of directional deformation on the energy spectra of layer crystals. The published experimental data on III–VI layer semiconductors will be discussed in the next subsection.

The absorption and luminescence spectra of GaSe, GaS, and InSe crystals were investigated[117-119] under uniaxial compression along the c axis ($p\|c$) and elongation along the layers ($p\perp c$) at temperatures in the range 5–150 K. The pressure did not exceed 2 kbar. The elasticity of the stresses was checked as follows: the absorption luminescence spectrum was recorded for an undeformed crystal and then it was recorded after deformation, and finally the spectrum of a free crystal was determined. The agreement between the first and third spectra was the criterion of the elastic nature of deformation.

Figure 20 shows the exciton absorption spectrum of GaSe at 5 K. The applied pressure $p\|c$ was up to 2 kbar. The absorption spectrum shown in Fig. 20 is characterized by exciton absorption lines corresponding to the $n = 1$ and $n = 2$ states. Compression clearly shifts the exciton absorption peaks toward higher energies and the shift is by the same amount of 4 meV. We can therefore say that the shifts of the exciton absorption bands are due to the changes in the direct band gaps. Figure 20 includes also the transmission spectrum of the same gallium selenide sample subjected to uniaxial stretching ($p\perp c$); clearly, elongation of a sample along the plane of the layers shifts the exciton absorption bands characterized by different values of n toward higher energies and the shift is of the same magnitude. Therefore, elongation of a sample in the direction of the layers reduces the direct band gap of GaSe.

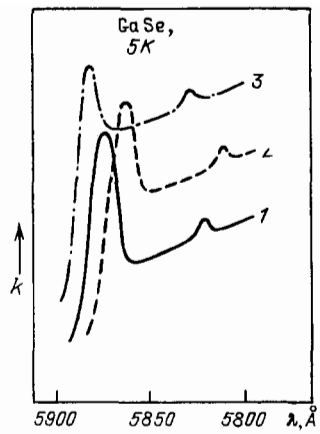

FIG. 20. Influence of uni-axial pressure on the spectrum of the direct exciton absorption in GaSe at low temperatures[117] 1) $p = 0$; 2) $\mathbf{p}\|c$; 3) $\mathbf{p}\perp c$.

The same conclusion can be reached from an analysis of the influence of pressure on the photoluminescence spectra of GaSe. Figure 21 shows the absorption spectrum of uniaxially ($p\|c$) deformed GaS. As in the case of GaSe, compression of a crystal by a pressure $p\|c$ shifts the exciton peak toward higher energies and at $p = 1$ kbar produces a shift of 5 meV. Elongation of GaS in the plane of the layers shifts the exciton absorption peak toward lower energies, exactly as in the case of GaSe. Similar results have been obtained in studies of the exciton absorption spectra of uniaxially deformed InSe; compression characterized by $p\|c$ increases E_g^d, whereas elongation reduces this value.

Information on the pressure dependences of the widths of the indirect band gaps of III–VI crystals is best obtained by investigating gallium sulfide. Since the experiments reported in Ref. 118 were carried out on thin gallium sulfide crystals, determination of the energy of the band gap E_g^i was

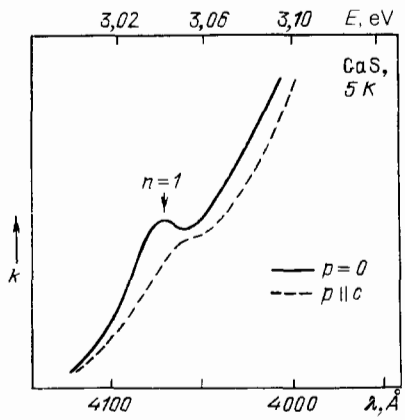

FIG. 21. Influence of uniaxial pressure on the spectrum of direct exciton absorption in GaS at low temperatures.[117]

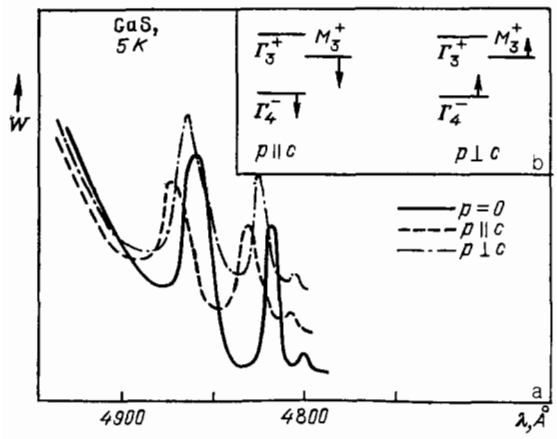

FIG. 22. a) Influence of uniaxial pressure on the spectrum of indirect exciton luminescence of GaS (Ref. 118). b) Shifts of energy bands due to uniaxial deformation in this layer crystal at low temperatures.[118]

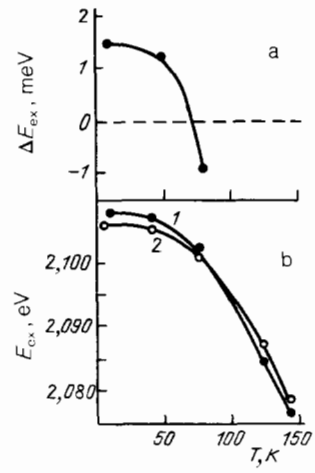

FIG. 23. a) Temperature dependence of the quantity $\Delta E_{ex} = E_{ex}(p\|c) - E_{ex}(p = 0)$ for GaSe (Ref. 119). b) Temperature dependence of E_{ex} for GaSe under pressure $p\|c$ (curve 1) and at $p = 0$ (curve 2), taken from Ref. 119.

carried out using an analysis of the luminescence spectra of eastically deformed and undeformed samples.

The radiation excited with light from a cw laser ($h\nu_{exc} = 2.80$ eV) was recorded from the surface of a layer of a single-crystal sample of gallium arsenide at 5 K (Fig. 22). The nature of the emission spectra of GaS has been established reliably.[121,122] The short-wavelength bands λ_2, λ_4, and λ_5 are due to radiative decay of indirect free and bound excitons accompanied by phonon emission. The line λ_2 is the result of decay of a free exciton accompanied by the emission of a $\hbar\omega = 10$ meV phonon. The lines λ_4 and λ_5 are due to the decay of a bound exciton accompanied by the emission of 10 and 30 meV phonons, respectively. We can clearly see the long-wavelength shift of the luminescence line as a result of uniaxial compression ($p\|c$) and elongation ($p\perp c$) of crystals. The band gap of gallium sulfide crystals in the case of indirect transitions ($\Gamma_4^- - M_3^+$) decreases in both cases (see the band structure in Fig. 16). When a sample is compressed along the c axis, the energy gap between the two conduction band minima of GaSe, GaS, and InSe crystals increases (Fig. 22b). This conclusion was confirmed by investigations of indium selenide.[118] The energy scheme in Fig. 22b demonstrates another important circumstance: the pressure coefficients $\partial E_g^i/\partial p$ are positive at 5 K under uniaxial deformation ($p\|c$) conditions, which is exactly opposite to the result observed under hydrostatic pressures at 300 K (Refs. 98 and 103). We recall that in the case of layer crystals the application of a uniaxial pressure $p\|c$ is practically equivalent to hydrostatic compression.

A full discussion of the experimental results should include the temperature dependences of the pressure coefficients of gallium selenide and its analogs. The relevant experimental data are plotted for GaSe in Figs. 23 and 24 (Ref. 119). Two types of experiments were carried out: in the former the absorption (luminescence) spectrum was recorded at a given temperature for an undeformed sample and then the pressure was applied and the value of $\Delta E = E_g^d(p \neq 0) - E_g^d(p = 0)$ was determined; the sample was unloaded and the same procedure was repeated at a different temperature (Fig. 23a). The second experiment involved a study of the temperature dependences of the energy positions of the exciton absorption peaks in a free crystal and the same crystal compressed along the c axis. Figure 23b shows the corresponding $E_{ex}(T)$ curves. The dependences $E_{ex}(T)$ intersected at $T \sim 80$ K. The results plotted in Fig. 23 demonstrate that at temperatures below 80 K the compression applied so that $p\|c$ increases E_g^d, whereas at temperatures 80 K it reduces E_g^d. Figure 24 shows the $E_{ex}(T)$ curves obtained for uniaxial elongation ($p\perp c$). We can clearly see that at this pressure the value of E_g^d decreases at all the investigated temperatures. In the case of gallium sulfide and indium selenide there is also an inversion of the sign of the pressure coefficient with temperature for the direct band gap when the pressure is applied so that $p\|c$ at temperatures in the region of ~ 80 K (Ref. 117).

If we now consider all the experimental data about the influence of pressure (hydrostatic or uniaxial) on the energy structure of the semiconductors GaS, GaSe, and InSe near the absorption edge, we find that some of the results cannot be understood on the basis of the simple band structure of GaSe (Ref. 79). This applies particularly to two effects exhibited by GaSe but unusual for semiconductors. These effects are the reversal of the sign of the pressure coefficients of $\partial E_g^d/\partial p$ with pressure (hydrostatic conditions, $T = 300$ K) or with temperature (uniaxial pressure $p\|c$, $p \sim 1$ kbar).

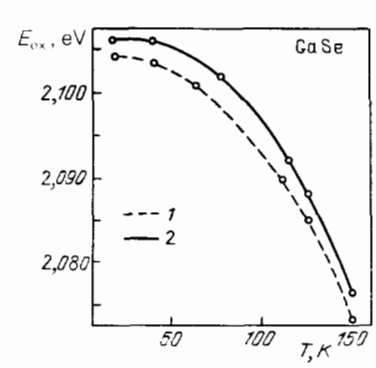

FIG. 24. Temperature dependence of the energy position of the exciton absorption peak of GaSe in the case when $p\perp c$ (curve 1) and $p = 0$ (curve 2).

We must discuss separately the dependence $E_g^d(p)$ obtained under hydrostatic pressures for gallium sulfide. We can understand qualitatively these effects if we bear in mind that gallium selenide and its analogs have a unit cell with atoms from two layers. The distances between the atoms within a layer (strong binding) and between the layers (weak binding) can vary in different ways with temperature and pressure. The contributions of the relevant strains (if they are considered separately) to the modification of the energy spectrum of a crystal under pressure can vary with temperature and pressure. This conclusion is well-grounded. We have mentioned earlier that in the case of graphite the elastic constants describing the interaction between the layers increase as a result of cooling faster than the intralayer elastic constants. On the other hand, when the pressure applied to a layer crystal is increased, the values of the elastic constants representing the interaction between atoms within the layers rise slowly, which corresponds to the interlayer constants (see Sec. 2.2).

In the next subsection we shall try to describe the deformation effects in layer crystals using the deformation potential model and allowing for the pressure and temperature dependences of the elastic constants.

4.4. Model of the deformation potential of layer semiconductors

Weak inhomogeneous deformation of a crystal can be described by the deformation tensor. The energy shift of a particular electron state in a crystal is generally governed by the deformation potential tensor. In the case of degenerate bands such deformation not only shifts the band as a whole, but may cause splitting of the bands as a result of partial or complete lifting of the degeneracy because of reduction in the symmetry. Consequently, changes in the spectrum as a result of deformation may be quite complex, as is true for example of the valence bands of germanium and silicon.[124]

In the case of layer III–VI semiconductor crystals the bands at the absorption edge are not degenerate because lowering of the symmetry does not play a decisive role in the course of deformation and in this sense the situation is simple. On the other hand, a classical analysis in which the strain tensor describes the change in a unit cell as a whole (relative displacements of the atoms within a cell are proportional to the load and are different for different atoms) does not always allow us to understand the nature of the deformation effects in layer semiconductors.

We shall consider the experimental results reported above using the deformation potential model. A simple energy band structure of GaSe and its analogs makes it possible to derive the following expression for the change in the band gap as a result of deformation:

$$\Delta E = D_{\parallel} \cdot u_{zz} + D_{\perp}(u_{xx} + u_{yy}). \qquad (4.1)$$

The deformation potentials $D_{\parallel}$ and $D_{\perp}$ can be found if the experimental results are used to find ΔE knowing the applied pressure p and if calculations are made of the values of the components of the strain tensors u_{zz}, u_{xx}, and u_{yy} at a given pressure using the relationships of the theory of elasticity. It is necessary to have data of two deformation experiments of different types.

We shall consider uniaxial elongation experiments when $p \perp c$ and those under hydrostatic compression carried out at room temperature and limited to pressures $p < 5$ kbar. In such cases the pressure coefficients $\partial E_g^d/\partial p$ are 10×10^{-6} eV/bar (Refs. 116 and 118) and -4×10^{-6} eV/bar (Refs. 98 and 101) in the case of gallium selenide. The negative sign of the pressure coefficient corresponds to a reduction in the band gap. Calculations of u_{zz}, u_{xx}, and u_{yy} with the aid of Table III and formulas (2.1) and (2.2) makes it possible to rewrite Eq. (4.1) in the form:

hydrostatic compression corresponds to

$$-4 \cdot 10^{-6} = -0.244 \cdot 10^{-5} D_{\parallel}^d - 0.106 \cdot 10^{-5} D_{\perp}^d,$$

whereas elongation corresponds to

$$-10 \cdot 10^{-6} = -0.028 \cdot 10^{-5} D_{\parallel}^d + 0.080 \cdot 10^{-5} D_{\perp}^d.$$

The calculated values of $D_{\parallel}^d$ and $D_{\perp}^d$ are $D_{\parallel}^d = +(6 \sim \pm 1)$ eV and $D_{\perp}^d = -(10 \pm 2)$ eV. The error in the deformation potentials governed by the error in the determination of the pressure coefficients and the components of the elasticity tensor. The values of $D_{\parallel}^d$ and $D_{\perp}^d$ have opposite signs: reduction in the dimensions of a crystal along the c axis reduces the width of the direct band gap E_g^d, whereas reduction in the dimensions in the plane of the layer increases E_g^d. For any other type of deformation the change in the band gap E_g^d will be governed by both effects. We can estimate the contribution of each of them under hydrostatic compression. It is found that ΔE_g^d is then governed by two quantities of similar magnitude but of opposite size, which is the reason for the relatively small values of the pressure coefficients $\partial E_g^d/\partial p$ in the case of crystalline analogs of gallium selenide (Table V). We can now understand the nature of inversion of these pressure coefficients as pressure is varied. In fact, at room temperature an increase in pressure increases the elastic constants of crystals and, consequently, alters the strains u_{zz}, u_{xx}, and u_{yy}. It is clear from the data in Sec. 2.2 that the elastic constant C_{33} representing the interaction between the layers rises more rapidly than C_{11} representing the interaction between atoms in a layer. Simple estimates obtained on the basis of Eq. (4.1) show that at pressures of ~ 5 kbar the positive term becomes larger than the negative term. The pressure coefficient then changes its sign.

We shall now find the deformation potentials using the experimental data on the influence of uniaxial deformations, such that $p \parallel c$ and $p \perp c$, on the value of E_g^d of GaSe at 5 K. The pressure coefficients are then $+2 \times 10^{-6}$ eV/bar and -10^{-5} eV/bar, respectively. We obtain

$$\text{for } p \parallel c: \quad 2 \cdot 10^{-6} = -0.299 \cdot 10^{-5} D_{\parallel}^d + 0.056 \cdot 10^{-5} D_{\perp}^d,$$

$$\text{for } p \perp c: \quad -10 \cdot 10^{-6} = -0.028 \cdot 10^{-5} D_{\parallel}^d + 0.080 \cdot 10^{-5} D_{\perp}^d.$$

The value $D_{\perp}^d = -(13 \pm 2)$ eV is almost the same as at room temperature, but $D_{\parallel}^d$ changes and becomes $-(3 \pm 1)$ eV. The deformation potential $D_{\parallel}^d$ shows a reversal of its sign with temperature. It should be pointed out that we always used the elastic constants listed in Table II and determined at room temperature. Therefore, there may have been errors in the calculations of these potentials. However, the components of the strain tensor may differ only in respect of the absolute value, whereas the signs of the deformation potentials governed by the signs of the corresponding pressure coefficients are definitely correct.

TABLE VI. Deformation potentials of GaSe-type layer crystals (eV).

Low T				High T			
$D_{\parallel}^{d}$	$D_{\perp}^{d}$	$D_{\parallel}^{i}$	$D_{\perp}^{i}$	$D_{\parallel}^{d}$	$D_{\perp}^{d}$	$D_{\parallel}^{i}$	$D_{\perp}^{i}$
-3 ± 1	-13 ± 2	0	-5 ± 1	$+6\pm1$	-10 ± 2	$+6\pm1$	-5 ± 1

We shall now consider the possible nature of the inversion of the sign of the deformation potential $D_{\parallel}^{d}$ of layer crystals with temperature. The results of theoretical calculations[79,125] demonstrate that the width of the band gap E_g^d increases on reduction in the thickness of a film of gallium selenide. On the other hand, cooling of layer crystals causes a more rapid rise of the elastic constants describing the interlayer coupling than of the intralayer constants [see Eq. (2.2)]. As pointed out already, the strain and deformation potentials apply usually to a unit cell as a whole. If we bear in mind that a unit cell of gallium selenide includes two layers, we can introduce phenomenologically two components of the strain tensor: u_{zz} (layer, denoted by lr) and u_{zz} (interlayer, denote by il). Introducing the notation u_{zz}^{lr}, u_{zz}^{il}, $D_{\parallel}^{lr}$, and $D_{\parallel}^{il}$, we can rewrite Eq. (4.1) in the form

$$\Delta E = (D_{\parallel}^{lr}\alpha_1 + D_{\parallel}^{il}\alpha_2)\, u_{zz} + D_{\perp}(u_{xx}+u_{yy}); \qquad (4.2)$$

here,

$$\alpha_1 = \frac{u_{zz}^{lr}}{u_{zz}}, \qquad \alpha_2 = \frac{u_{zz}^{il}}{u_{zz}}, \qquad \alpha_1+\alpha_2 = 1.$$

Cooling at a given pressure increases α_1 and reduces α_2. Bearing in mind that $D_{\parallel}^{lr}<0$ and $D_{\parallel}^{d}>0$, we can understand the inversion of the sign of $D_{\parallel}^{c}$ with temperature.

When a layer crystal of gallium selenide is deformed, at low temperatures the main contribution to E_g^d comes from the change in the distances between the atoms within a layer. At high temperatures $T>80$ K the main role is played by the interlayer distances.

We have discussed so far the deformation potentials describing the change in the direct band gap with pressure. Similar considerations apply also to the case of indirect transitions. Table VI gives the deformation potentials calculated from the experimental results. A comparison with theoretical calculations[125] shows that the agreement is satisfactory. An analysis of the data in Table VI demonstrates that the relatively high values of $|\partial E_g^i/\partial p|$ are due to the smallness of $D_{\perp}^{i}$. In view of this, the second term of Eq. (4.2), which makes a positive contribution to ΔE, is small. For this reason the reduction in u_{zz} on increase in pressure does not result in inversion of the sign of the pressure coefficients.

All these discussions and the numerical data given above on direct transitions apply to gallium selenide, whereas those on indirect transitions apply to gallium sulfide. However, it is stressed in Ref. 118 that the general picture of the deformation effects does not vary along the series of crystals GaSe, GaS, and InSe. Since the polytypic composition of the investigated crystals is clearly different [see Eq. (2.1)], this observation shows that the differences between the deformation potentials of crystals of different polytypes are small. Experimental evidence is available on the equality of the pressure coefficients of GaSe crystals of different polytypic compositions.[102]

5. CONCLUSIONS

It was not the purpose of the present review to provide an exhaustive account of all the experimental results obtained in studies of the influence of pressure on the properties of numerous layer crystals. The review has been concerned mainly with the effects which are characteristic of the crystal structure of layer materials with a weak interlayer interaction. The topics considered in this review do not represent a special chapter of the physics of crystals with a weak coupling, but are related in our opinion, to some of the new effects discovered recently. We have in mind here structural phase transitions which appear in layer crystals under pressure,[7,9,99] ferroelectric phase transitions as a result of a change in temperature [126] low-temperature (4.2 K) plastic flow of gallium selenide not in the basal plane (parallel to the layers) but in a pyramidal plane oriented at an angle to the plane of the layers.[127]

Information on the temperature-dependence of the components of the strain tensor and on the magnitudes of the deformation potentials makes it possible to separate the contributions which are made to the experimentally established temperature dependences by the energies of electron and phonon states due to thermal expansion, on the one hand, and to the intrinsic part of the electron-phonon and phonon-phonon interactions, on the other. Such an analysis has made it possible, for example, to reveal the low-temperature features of the electron-phonon interaction in gallium sulfide.[128] Knowing the deformation potentials, it became possible to demonstrate the applicability of the model of a virtual crystal[129] to the case of solid solutions of layer semiconductors; this information will be useful in studies of the energy structure of heterojunctions formed from layer crystals.[130,131]

Finally, the question of the nature of changes in the energy spectrum of a crystal due to changes in the distances between the layers is undoubtedly relevant to the branch of the physics of layer crystals which continues to develop and which is concerned with intercalated compounds (see, for example, Ref. 132).

The authors regard it as their pleasant duty to thank A. A. Abrikosov and D. E. Khmel'nitskiĭ, conversations with whom stimulated the writing of the present review, and N. A. Abdullaev for his help in the preparation of the text.

[1]G. L. Belen'kiĭ and V. B. Stopachinskiĭ, Usp. Fiz. Nauk **140**, 233 (1983) [Sov. Phys. Usp. **26**, 497 (1983)].
[2]I. M. Lifshitz, Zh. Eksp. Teor. Fiz. **22**, 475 (1952).
[3]F. Levy, Nuovo Cimento B **38**, 359 (1977).
[4]R. W. G. Wyckoff, *Crystal Structures*, Vol. 1, Interscience, New York (1963).
[5]R. S. Pease, Acta Crystallogr. **5**, 356 (1952).

[6]A. Kuhn, A. Chevy, and R. Chevalier, Phys. Status Solidi A **3**,1 469 (1975).
[7]H. D'Amour, W. B. Holzapfel, A. Polian and A. Chevy, Solid State Commun. **44**, 853 (1982).
[8]S. A. Semiletov, Kristallografiya **3**, 288 (1958) [Sov. Phys. Crystallogr. **3**, 292 (1958)].
[9]H. Shinriki, K. Takemura, K. Asaumi, and S. Minomura, in: High Pressure in Research and Industry (Proc. Eighth Intern. Conf. on Research in High Pressure Science and Technology and Nineteenth Conf. of European High Pressure Research Group, Uppsala, 1981, ed. by C. M. Backman, T. Johannisson, and L. Tegner), Vol. 2, p. 540.
[10]J. C. Bowman and J. A. Krumhansl, J. Phys. Chem. Solids **6**, 367 (1958).
[11]G. Dolling and B. N. Brockhouse, Phys. Rev. B **128**, 1120 (1962).
[12]W. B. Gauster, Philos. Mag. **25**, 687 (1972).
[13]K. Komatsu, J. Phys. Chem. Solids **6**, 380 (1958).
[14]K. Komatsu, J. Phys. Chem. Solids **25**, 707 (1964).
[15]O. L. Blakslee, D. G. Proctor, E. J. Seldin, G. B. Spence, and T. Weng, J. Appl. Phys. **41**, 3373 (1970).
[16]E. J. Seldin and C. W. Nezbeda, J. Appl. Phys. **41**, 3389 (1970).
[17]B. M. Powell, S. Jandl, J. L. Brebner, and F. Levy, J. Phys. C **10**, 3039 (1977).
[18]A. Polian, J. M. Besson, M. Grimsditch, and H. Vogt, Appl. Phys. Lett. **38**, 334 (1981).
[19]C. Hamaguchi, K. Wasa, and M. Yamawaki, Proc. Third Intern. Conf. on Phonon Scattering in Condensed Matter, Providence, RI, 1979, publ. by Plenum Press, New York (1980), p. 441.
[20]S. Adachi and C. Hamaguchi, Solid State Commun. **31**, 245 (1979).
[21]M. Gatulle, M. Fischer, and A. Chevy, Phys. Status Solidi B **119**, 327 (1983).
[22]M. Tanaka, M. Yamada, and C. Hamaguchi, J. Phys. Soc. Jpn. **38**, 1708 (1975).
[23]T. C. Chiang, J. Dumas, and Y. R. Shen, Solid State Commun. **28**, 173 (1978).
[24]Kh. M. Khalilov and K. N. Rzaev, Kristallografiya **11**, 929 (1966) [Sov. Phys. Crystallogr. **11**, 786 (1967)].
[25]V. M. Kovtun and V. P. Mikhal'chenko, Izv. Akad. Nauk SSSR Neorg. Mater. **16**, 1203 (1980).
[26]Z. A. Iskender-Zade, V. D. Faradzhev, and A. I. Agaev, Fiz. Tverd. Tela (Leningrad) **19**, 851 (1977) [Sov. Phys. Solid State **19**, 492 (1977)].
[27]W. G. Stirling, B. Dorner, J. D. N. Cheeke, and J. Revelli, Solid State Commun. **18**, 931 (1976).
[28]D. E. Moncton, J. D. Axe, and F. J. Di Salvo, Phys. Rev. B **16**, 801 (1977).
[29]J. L. Brebner, S. Jandl, and B. M. Powell, Nuovo Cimento B **38**, 263 (1977).
[30]J. F. Green, P. Bolsaitis, and I. L. Spain, J. Phys. Chem. Solids **34**, 1927 (1973).
[31]W. B. Gauster and I. J. Fritz, J. Appl. Phys. **45**, 3309 (1974).
[32]A. Polian, J. M. Besson, M. Grimsditch, and H. Vogt, Phys. Rev. B **25**, 2767 (1982).
[33]J. A. Reissland, *The Physics of Phonons*, Wiley, New York (1973) [Russ. transl., Mir, M., 1975].
[34]L. D. Landau and E. M. Lifshitz, *Theory of Elasticity*, 2nd ed. Pergamon Press, Oxford (1970) [Russ. original, Nauke, M., 1965].
[35]F. S. Crawford Jr, *Waves* (Berkeley Physics Course), McGraw-Hill New York (1968) [Russ. Transl., Nauka, M., 1974].
[36]A. M. Kosevich, Physical Mechanics of Real Crystals [in Russian], Naukova Dumka, Kiev (1981).
[37]R. M. Niclow, N. Wakabayashi, and H. G. Smith, Phys. Rev. B **5**, 4951 (1972).
[38]N. Wakabayashi, H. G. Switch, and R. M. Niclow, Phys. Rev. B **12**, 659 (1975).
[39]N. Wakabayashi, Nuovo Cimento B **38**, 256 (1977).
[40]S. Jandl, J. L. Brebner, and B. M. Powell, Phys. Rev. B **13**, 686 (1976).
[41]R. Zallen, M. L. Slade, and A. T. Ward, Phys. Rev. B **3**, 4257 (1971).
[42]M. P. Lisitsa, A. M. Yaremko, G. G. Tarasov, M. Ya Valakh, and L. I. Berezhinskiĭ, Fiz. Tverd. Tela (Leningrad) **14**, 3219 (1972) [Sov. Phys. Solid State **14**, 2744 (1973)].
[43]J. L. Verble, T. J. Wieting, and P. R. Reed, Solid State Commun. **11**, 941 (1972).
[44]T. J. Wieting and J. L. Verble, Phys. Rev. B **5**, 1473 (1972).
[45]M. Hayek, O. Brafman, and R. A. M. Lieth, Phys. Rev. B **8**, 2772 (1973).
[46]L. N. Alieva, G. L. Belen'kiĭ, I. I. Reshina, É. Yu. Salaev, and V. Ya. Shteĭnshraĭber, Fiz. Tverd. Tela (Leningrad) **21**, 155 (1979) [Sov. Phys. Solid State **21**, 90 (1979)].
[47]J. M. Besson, R. Le Toullec, J. P. Pinceaux, A. Chevy, and H. Fair, High Temp. High Press. **7**, 710 (1975).
[48]E. A. Vinogradov, G. N. Zhizhin, N. N. Melnik, S. I. Subbotin, V. V. Panfilov, K. R. Allakhverdiev, S. S. Babaev, and V. F. Zhitar, Phys. Status Solidi B **99**, 215 (1980).
[49]R. Zallen, Phys. Rev. B **9**, 4485 (1974).
[50]E. A. Vinogradov, N. M. Gasanly, A. F. Goncharov, G. N. Zhizhin, N. N. Mel'nik, V. V. Panfilov, A. S. Ragimov, and S. I. Subbotin, Fiz. Tverd. Tela (Leningrad) **24**, 139 (1982) [Sov. Phys. Solid State **24**, 77 (1982)].
[51]G. Martinez, in: *Handbook on Semiconductors* (gen. ed. T. S. Moss), Vol. 2, Optical Properties of Solids (ed. by M. Balkanski), North-Holland, Amsterdam (1980), p. 181.
[52]A. Polian, K. Kunc, R. Le Toullec, and B. Dorner, Proc. Fourteenth Intern. Conf. on Physics of Semiconductors, Edinburgh, 1978, publ. by Institute of Physics, London (1979), p. 907.
[53]N. A. Abdullaev, L. N. Alieva, and R. A. Suleĭmanov, Phys. Status Solidi B **129**, K13 (1985).
[54]R. Zallen and E. M. Conwell, Solid State Commun. **31**, 557 (1979).
[55]L. D. Landau and E. M. Lifshitz, *Statistical Physics*, 2nd. ed., Pergamon Press, Oxford (1969) [Russ. original, Nauka, M., 1964].
[56]S. I. Novikova, Thermal Expansion of Solids [in Russian], Nauka, Moscow (1974).
[57]T. H. K. Barron, J. G. Collins, and G. K. White, Adv. Phys. **29**, 609 (1980).
[58]J. B. Nelson and D. P. Riley, Proc. Phys. Soc. London **57**, 477 (1945).
[59]E. Matuyama, Tanso **7**, 12 (1958).
[60]E. G. Steward and B. P. Cook, Nature (London) **185**, 78 (1960).
[61]F. Entwisle, Phys. Lett. **2**, 236 (1962).
[62]A. C. Bailey and B. Yates, J. Appl. Phys. **41**, 5088 (1970).
[63]B. Yates, H. J. Overy, and O. Pirgon, Philos. Mag. **32**, 847 (1975).
[64]E. A. Kellett and B. P. Richards, J. Appl. Crystallogr. **4**, 1 (1971).
[65]S. E. Hardcastle and H. Zabel, Phys. Rev. B **27**, 6363 (1983).
[66]B. T. Kelly and P. L. Walker Jr, Carbon **8**, 211 (1970).
[67]R. W. Munn, J. Phys. C **5**, 535 (1972).
[68]N. G. Aliev, I. G. Kerimov, M. M. Kurbanov, and T. A. Mamedov, Fiz. Tverd. Tela (Leningrad) **14**, 1522 (1972) [Sov. Phys. Solid State **14**, 1304 (1972)].
[69]G. L. Belen'kiĭ, S. G. Abdullaeva (Abdullayeva), A. V. Solodukhin and R. A. Suleĭmanov (Suleymanov), Solid State Commun. **44**, 1613 (1982).
[70]G. L. Belen'kiĭ, R. A. Suleĭmanov, N. A. Abdullaev, and V. Ya. Shteĭnshraĭber, Fiz. Tverd. Tela (Leningrad) **26**, 3560 (1984) [Sov. Phys. Solid State **26**, 2142 (1984)].
[71]Yu. A. Kovalevskaya and P. G. Strelkov, Fiz. Tverd. Tela (Leningrad) **8**, 1302 (1966) [Sov. Phys. Solid State **8**, 1044 (1966)].
[72]N. A. Abdullaev, K. R. Allakhverdiev, G. L. Belen'kiĭ, T. G. Mamedov, R. A. Suleĭmanov, and Ya. N. Sharifov, Solid State Commun. **53**, 601 (1985).
[73]F. L. Givens and G. E. Fredericks, J. Phys. Chem. Solids **38**, 1363 (1977).
[74]A. M. Simpson, M. H. Jericho, and F. J. Di Salvo, Solid State Commun. **44**, 1543 (1982).
[75]G. L. Belen'kiĭ, E. Yu. Salaev, R. A. Suleĭmanov, N. A. Abdullaev, and V. Ya. Shteĭnshraĭber, Solid State Commun. **53**, 967 (1985).
[76]B. T. Kelly, Philos. Mag. **32**, 859 (1975).
[77]S. I. Novikova, Fiz. Tverd. Tela (Leningrad) **10**, 3439 (1968) [Sov. Phys. Solid State **10**, 2723 (1969)].
[78]R. D. McCammon and G. K. White, Philos. Mag. **11**, 1125 (1965).
[79]M. Schluter, Nuovo Cimento B **13**, 313 (1973).
[80]Y. Depeursinge, Nuovo Cimento B **38**, 153 (1977).
[81]J. V. McCanny and R. B. Murray, J. Phys. C **10**, 1211 (1977).
[82]F. M. Gashimzade, D. A. Guseĭnova, and D. G. Guliev, Fiz. Tverd. Tela (Leningrad) **27**, 2098 (1985) [Sov. Phys. Solid State **27**, 1257 (1985)].
[83]H. Kamimura and K. Nakao, J. Phys. Soc. Jpn. **24**, 1313 (1968).
[84]F. Bassani and G. Pastori-Parravicini, Nuovo Cimento B **50**, 95 (1967).
[85]V. S. Bagaev, G. L. Belen'kiĭ, V. V. Zaĭtsev, É. Yu. Salaev, and V. B. Stopachinskiĭ, Fiz. Tverd. Tela (Leningrad) **21**, 2217 (1979) [Sov. Phys. Solid State **21**, 1275 (1979)].
[86]C. H. Aldrich, C. M. Fowler, R. S. Caird, W. B. Garn, and W. G. Witteman, Phys. Rev. B **23**, 3970 (1981); G. Ottaviani, C. Canali, F. Nava, Ph. Schmid, E. Mooser, R. Minder, I. Zschokke, Solid State Commun. **14**, 933 (1974).
[87]E. Mooser and M. Schluter, Nuovo Cimento B **18**, 164 (1973).
[88]Y. Depeursinge, E. Doni, R. Girlanda, A. Baldereschi, and K. Maschke, Solid State Commun. **27**, 1449 (1978).
[89]J. Camassel, P. Merle, H. Mathieu, and A. Chevy, Phys. Rev. B **17**, 4718 (1978).
[90]M. V. Andriyashik, M. Yu. Sakhnovskii, V. B. Timofeev, and A. S.

Yakimova, Phys. Status Solidi **28**, 277 (1968).
[91]E. Aulich, J. L. Brebner, and E. Mooser, Phys. Status Solidi **31**, 129 (1969).
[92]P. K. Larsen, M. Schluter, N. V. Smith, Solid State Commun. **21**, 775 (1977).
[93]P. K. Larsen, S. Chiang, and N. V. Smith, Phys. Rev. B **15**, 3200 (1977).
[94]G. Margaritondo, J. E. Rowe, and S. B. Christman, Phys. Rev. B **15**, 3844 (1977).
[95]G. Margaritondo, J. E. Rowe, and H. Kasper, Nuovo Cimento B **38**, 234 (1977).
[96]S. I. Subbotin, V. V. Panfilov, L. F. Vereshchagin, R. T. Molchanova, and G. A. Akhundov, Dokl. Akad. Nauk SSSR **202**, 1039 (1972) [Sov. Phys. Dokl. **17**, 126 (1972)].
[97]V. V. Panfilov, S. I. Subbotin, and L. F. Vereshchagin, Dokl. Akad. Nauk SSSR **196**, 559 (1971) [Sov. Phys. Dokl. **16**, 24 (1971)].
[98]V. V. Panfilov, S. I. Subbotin, L. F. Vereshchagin, I. I. Ivanov, and R. T. Molchanova, Phys. Status Solidi B **72**, 823 (1975).
[99]S. I. Subbotin, V. V. Panfilov, and R. T. Molchanova, Phys. Status Solidi A **39**, 357 (1977).
[100]J. M. Besson, Nuovo Cimento B **38**, 478 (1977).
[101]J. M. Besson, R. Le Toullec, J. P. Pinceaux, A. Chevy, and H. Fair, Proc. Fifth Intern. Conf. on High Pressure Physiscs and Technology, Moscow, 1975, in: High Temp. High Press. **7**, 710 (1975).
[102]M. Mejatty, A. Segura, R. Le Toullec, J. M. Besson, A. Chevy, and H. Fair, J. Phys. Chem. Solids **39**, 25 (1978).
[103]J. M. Besson, K. P. Jain, and A. Kuhn, Phys. Rev. Lett. **32**, 936 (1974).
[104]A. S. Davydov, *Theory of Molecular Excitons*, Plenum Press, New York (1971) [Russ. original, Nauka, M., 1968].
[105]A. J. Grant, J. A. Wilson, and A. D. Yoffe, Philos. Mag. **25**, 625 (1972).
[106]G. R. Valyukonis, D. A. Guseĭnova, G. Z. Krivaĭte, and A. Yu. Shileĭka, Fiz. Tekh. Poluprovodn. **19**, 282 (1985) [Sov. Phys. Semicond. 19, 173 (1985)].
[107]M J. Powell and A. J. Grant, Nuovo Cimento B **38**, 486 (1977).
[108]G. Valyukonis (Valiukonis), G. Krivaĭte, D. I. Bletskan, and A. Shileĭka (Sileika), Phys. Status Solidi B **128**, K37 (1985).
[109]L. F. Mattheiss Phys. Rev. B **8**, 3719 (1973).
[110]I. C. Schluter and M. Schluter, Phys. Status Solidi B **57**, 145 (1973).
[111]I. C. Schluter and M. Schluter, Phys. Rev. B **9**, 1652 (1974).
[112]D. K. Wright and M. R. Tubbs, Phys. Status Solidi **37**, 551 (1970).
[113]J. B. Anthony and A. D. Brothers, Phys. Rev. B **7**, 1539 (1973).
[114]A. D. Brothers and J. T. Pajor, Phys. Rev. B **14**, 4570 (1976).
[115]C. Carillon and G. Martinez, Nuovo Cimento B **38**, 496 (1977).
[116]N. P. Gavaleshko, M. V. Kurik, G. B. Delevskiĭ, Z. D. Kovalyuk, A. I. Savchuk, and I. F. Skitsko, Ukr. Fiz. Zh. **19**, 1741 (1974).
[117]G. L. Belen'kiĭ, É. Yu. Salaev, R. A. Suleĭmanov, and É. I. Mirzoev, Phys. Status Solidi A **63**, 97 (1981).
[118]G. L. Belen'kiĭ and R. A. Suleĭmanov, Solid State Commun. **41**, 549 (1982).
[119]G. L. Belen'kiĭ, É. Yu. Salaev, R. A. Suleĭmanov, and É. I. Mirzoev, Fiz. Tverd. Tela (Leningrad) **22**, 3153 (1980) [Sov. Phys. Solid State **22**, 1842 (1980)].
[120]Y. Sasaki, K. Hoshi, S. Saito, K. Yamaguchi, and Y. Nishina, J. Phys. Soc. Jpn. **52**, 3706 (1983).
[121]G. L. Belen'kiĭ and M. O. Godzhaev, Phys. Status Solidi B **85**, 453 (1978).
[122]G. L. Belen'kiĭ, M. O. Godzhaev, and É. Yu. Salaev, Pis'ma Zh. Eksp. Teor. Fiz. **26**, 385 (1977) [JETP Lett. **26**, 263 (1977)].
[123]B. S. Razbirin, M. I. Karaman, V. P. Mushinskiĭ, and A. N. Starukhin, Fiz. Tekh. Poluprovodn. **7**, 1112 (1973) [Sov. Phys. Solid State **7**, 753 (1973)].
[124]G. L. Bir and G. E. Pikus, *Symmetry and Strain-Induced Effects in Semiconductors*, Israel Program for Scientific Translations, Jerusalem; Wiley, New York (1975) [Russ. original, Nauka, M., 1972].
[125]T. R. Mekhtiev and S. M. Ragimova, Deposited Paper No. 6394-83 [in Russian], VINITI, Moscow (1983).
[126]R. A. Aliev, K. R. Allakhverdiev, A. I. Baranov, N. R. Ivanov, and R. M. Sardarly, Fiz. Tverd. Tela (Leningrad) **26**, 1271 (1984) [Sov. Phys. Solid State **26**, 775 (1984)].
[127]G. L. Belen'kiĭ, V. A. Goncharov, V. D. Negriĭ, Yu. A. Osip'yan, and R. A. Suleĭmanov, Fiz. Tverd. Tela (Leningrad) **26**, 3145 (1984) [Sov. Phys. Solid State **26**, 1893 (1984)].
[128]G L. Belen'kiĭ, É. Yu. Salaev, R. A. Suleĭmanov, and N. A. Abdullaev, Solid State Commun. **47**, 263 (1983).
[129]G. L. Belen'kiĭ and R. A. Suleĭmanov, Fiz. Tverd. Tela (Leningrad) **26**, 3706 (1984) [Sov. Phys. Solid State **26**, 2233 (1984)].
[130]R. Spah, U. Elrod, M. Lux-Steiner, E. Bucher, and S. Wagner, Appl. Phys. Lett. **43**, 79 (1983).
[131]R. Spah, M. Lux-Steiner, and E. Bucher, Appl. Phys. Lett. **45**, 744 (1984).
[132]R. Clarke and C. Uber, Adv. Phys. **33**, 469 (1984).

Translated by A. Tybulewicz